Laser source for multiple wavelength interferometry

Finn Klemming Eklöf

Master thesis in Physics

Laser Physics
Department of Applied Physics
School of Engineering Science
KTH

Stockholm, Sweden 2014

To Monkey

Peanut

And the long road that led here.

Laser source for multiple wavelength interferometry

Laser Physics
Department of Applied Physics
KTH – Royal Institute of Technology
10691 Stockholm
Sweden

TRITA-FYS 2015:23
ISSN 0280-316X
ISRN KTH/FYS/--15:23—SE

Abstract

This thesis describes the work at the Royal Institute of Technology on the conception and construction of a multi-wavelength laser, to be used in digital holography experiments at Luleå Technical University. The stated goal was to create a system that could simultaneously deliver several laser beams at different wavelengths without the need for wavelength tuning or other manipulation that could at the same time be used in a harsh industrial environment. The first part describes the creation and discussion of several ideas and theoretically possible systems. These ideas were evaluated in several rounds of discussions after which a decision to construct a specific prototype was made. The second part describes the practical work from constructing the first miniature test beds to the finalization of a working and tested system.

Sammanfattning

Föreliggande avhandling beskriver arbetet vid KTH med att utforma och konstruera en flervåglängds laser, avsedd att användas i digital holografi experiment vid Luleå Tekniska Universitet. Det uttalade målet var att skapa ett system som samtidigt kunde leverera flera laserstrålar på olika våglängder utan behov av inställning eller annan manipulering och som samtidigt skall kunna användas i en hård och krävande industrimiljö. Den första delen är en diskussion av flera idéer och teoretiskt möjliga system. Dessa idéer utvärderades i flera omgångar av diskussioner varefter ett beslut att bygga en specifik prototyp gjordes. Den andra delen beskriver det praktiska arbetet från att bygga de första miniatyrtestbäddar till slutförandet av ett fungerande och testat system.

Acknowledgements

My gratitude goes out to all those involved in the span of this work. Be it as a technical advisor, a facilitator of means or a supporting voice during long hours in dark laboratories.

In no particular order:

Fredrik Laurell

Walter Margulis

Emil Hällstig

Staffan Tjörnhammar

Patrik Holmberg

Peter Zeil

Nicky Thilmann

Hoon Jang

Patrik Rugeland

Mikael Malmström

Zhangwei Yu

You all played a part, big or small, and I thank you with love.

Contents

1 Introduction

Today laser interferometry and holography are both well-known and commonly used methods for measuring e.g. distance, position, vibrations, deformations, pressure or index of refraction with very high accuracy. The use of these methods can be found all around society and can be as common as a price tag scanner or used in industry, hospitals or laboratories. One of several strengths of these methods is the use of the wavelengths of light as reference. This allows for measuring with very high precision. However, it introduces a problem when trying to measure larger discontinuities, surfaces, objects or changes. Interferometry relies on the difference in optical path lengths between two optical arms resulting in a measurable phase difference. Due to the periodic nature of the electromagnetic field, resolution of phase difference in interferometry is limited to a 2π interval. This is called a $2\pi-$phase ambiguity and is common in other fields, for example GPS-positioning. Phase differences outside of the 2π range are wrapped back into this interval, i.e. it is impossible to distinguish between π and 3π phase difference resulting in an unambiguous measuring length of half the measuring wavelength ($\lambda/2$) [1]. A common approach to circumvent this issue and to enable high depth resolution imaging is to evaluate multiple interferometric measurements at different wavelengths. The phase difference between two interferometer phases, obtained from measurements at different wavelengths act like a single phase with a corresponding "synthetic" wavelength longer than the individual wavelengths used [1]. Using several synthetic wavelengths and repeating the process it is possible to effectively synthesize even longer unambiguous lengths, enabling measurements of much larger lengths or depths [1-3].

Clear imaging i.e. avoiding noise in measurements, puts high demands on any light source used. Specifically high temporal and spatial coherence are desirable. Fiber lasers lend themselves particularly well to these demands. The research and industrial fields of fiber lasers and optical fibers have grown significantly over the past years and the advantages of such systems are considerable. For example, fiber lasers are often chosen because of their ability to deliver high output power and optical quality, their compact size, reliable long term operation, and flexible design options.

Luleå Technical University [LTH] have a long and tried experience with different measurement techniques. Among these they have enjoyed particular success with pulsed laser systems. Therefore there is considered to be great potential in a pulsed laser source that is capable of simultaneous delivery of coherent light at several different wavelengths.

The results of this project will have a direct influence on a parallel research project financed by Vinnova aiming to make accurate 3D-measurements for geometric evaluation in large scale industry.

The objective of the work

The main goal of the work presented in this thesis was to construct and evaluate a multi-wavelength laser to be used in an experimental setup for 3D-imaging. Several criteria set by Luleå Technical University and Optronic on the system were taken into consideration. Firstly the laser should be as simple as possible, meaning it should be potentially cheap to build in larger volumes. Second, it should be transverse and longitudinally single mode. Furthermore it would be ideal if it was possible to scale the system to deliver 10 to 15 separate wavelengths spectrally separated by 1nm. It should be possible to synchronically pulse the lasers in 1µs pulses with about 0.1mJ pulse energy per wavelength. Lastly the light should be visible or near infrared wavelengths to facilitate the use of common commercial detectors.

The work consisted of two parts. The first part was a concept study to find and evaluate possible options for laser systems to be built. When an agreeable solution was found, as the second part of the work, the chosen system was built as a first prototype and sent to LTH for evaluation.

2 THEORY

2.1 The Laser

2.1.1 Background

The Laser, a device based on *L*ight *A*mplification by *S*timulated *E*mission of *R*adiation, first saw the light of day in 1957. Conceptually a laser can be said to generally consist of three mandatory components. The *gain medium* is a material with atomic and structural properties suitable for generating and amplifying specific electromagnetic waves. The *pump* is a means to feed energy to the *gain medium* in order to excite specific quantized energy levels to achieve light generation. This is normally done by using another light source such as a laser or flash lamp, or an electric potential. The *cavity* is a feedback system to ensure amplification, often at some desired specific wavelength. Normally the cavity consists of dielectric mirrors or Bragg gratings or both.

2.1.2 Principle

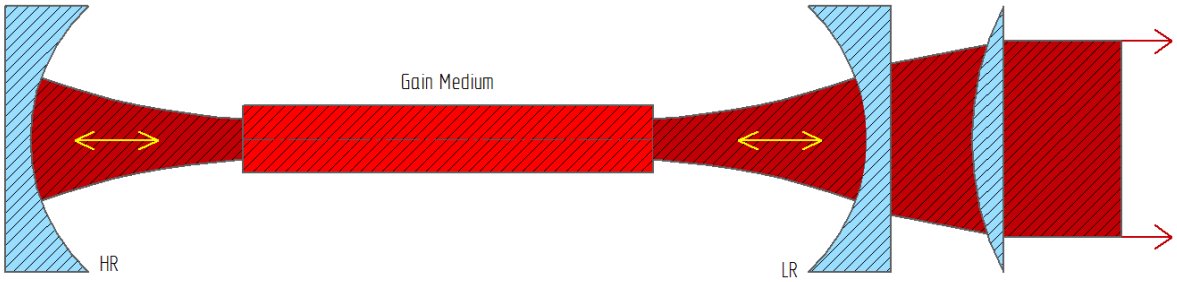

Figure 2.1. An illustrative drawing of the main components of a laser. HR and LR are high and low reflectors respectively.

Light emitted by a laser is governed by the rules of quantum mechanics that limit any system of particles to discrete energy levels. A photon, having strictly defined energy quanta, passing through the gain medium will excite a particle from a lower state of energy to a higher. Alternatively de-excite the particle from a higher to a lower state forcing it to emit a photon of the same phase and wavelength as the incident wave if such a matching transition is available. The latter is generally referred to as *stimulated emission,* as opposed to *spontaneous emission* where a particle decays, with random phase and wavelength, without external influence.

Amplification is achieved by pumping the gain medium, often with another laser to force a high population of excited states. A higher amount of particles in their excited state compared to some other lower state is called *population inversion* and will cause the probability

of a photon to be emitted to be higher than being absorbed, hence amplifying light passing through the medium.

When an amplifier such as the one described above is placed inside a resonant optical cavity, a laser oscillator is born. As depicted in Fig. 2.1 the cavity generally consists of two mirrors, one with high reflectivity, and the other (the output coupler, or OC for short) with lower reflectivity e.g. 90% forcing the average photon to pass back and forth several times through the gain medium ensuring large amplification. This amplified light, i.e. the laser beam, is transmitted through the output coupler.

As the light is reflected several times standing waves are formed inside the cavity. These are the result of constructive interference of radiation that fulfils the criteria of:

$$q\frac{\lambda}{2} = L, \tag{2.1}$$

where q is an integer, λ is the wavelength of the radiation field and L is the cavity optical path length. This ensures that a particular wave will have a node at the end mirrors and consequently be reproduced. Fields fulfilling this criterion are called *longitudinal modes* since they are axial modes along the cavity optical axis (z-axis, beam propagation axis). All other fields will interfere destructively. This is what ensures the quasi monochromaticity of a laser since the cavity will select a distinct set of wavelengths out of the gain mediums broader emission bandwidth. The number of longitudinal modes is the limiting factor on temporal coherence. The fewer longitudinal modes there are the longer the coherence length will be and the narrower the resulting lasers output spectrum. One way of ensuring a working, single longitudinal mode laser, is to ensure that the mode spacing is such that

$$\frac{c}{2L} = \Delta v \tag{2.2}$$

exceed the transmission bandwidth of the gain medium. Here c is the speed of light in vacuum and Δv is the frequency separation between two longitudinal modes. This ensures that only one mode within the emission bandwidth will experience gain. Eq. 2.2 shows that to achieve large mode spacing, a short cavity length is needed. A short cavity however, implies a shorter length of gain medium can be used than in a longer cavity. A shorter piece of gain medium means that light incident on the gain medium sees less actual available electrons to excite per pass resulting in a lower power efficiency and generally lower output power for a given pump source.

The spatial coherence of the laser is governed by the *T*ransverse *E*lectro*M*agnetic modes, TEM modes. These are modes nearly normal to the z-axis and are caused by the distortion of an ideally planar wave front due to different diffraction phenomena in the cavity. For a square waveguide, such as a slab of sapphire these are described by the intensity profile[4]:

$$I_{mn}(x,y,z) = I_0\left[\left(H_m\frac{\sqrt{2}x}{w}\right)exp\left(-\frac{x^2}{w^2}\right)\right]^2\left[\left(H_n\frac{\sqrt{2}y}{w}\right)exp\left(-\frac{y^2}{w^2}\right)\right]^2 \quad (2.3)$$

Here I_0 is the maximum intensity, $H_{m,n}$ is the Hermite polynomials, ω is the beam radius and x and y are the transverse directions to the beam propagation axis.

Alternately it is of interest to look at the intensity profile in polar coordinates which is the case of cylindrical waveguides as in, for example, optical fibers. The corresponding intensity profile is then given by:

$$I_{pl}(\rho,\varphi) = I_0\rho^l\left[L_p^l(\rho)\right]^2\cos^2(l\varphi)e^{-\rho} \quad (2.4)$$

where L_p^l is the Laguerre polynomials, p and l are integers labelling the radial and angular mode orders and $\rho = \frac{2r}{w}$ where w is the spot size corresponding to the Gaussian mode beam radius. Fig. 2.2 shows the intensity profiles of the lowest ordered modes.

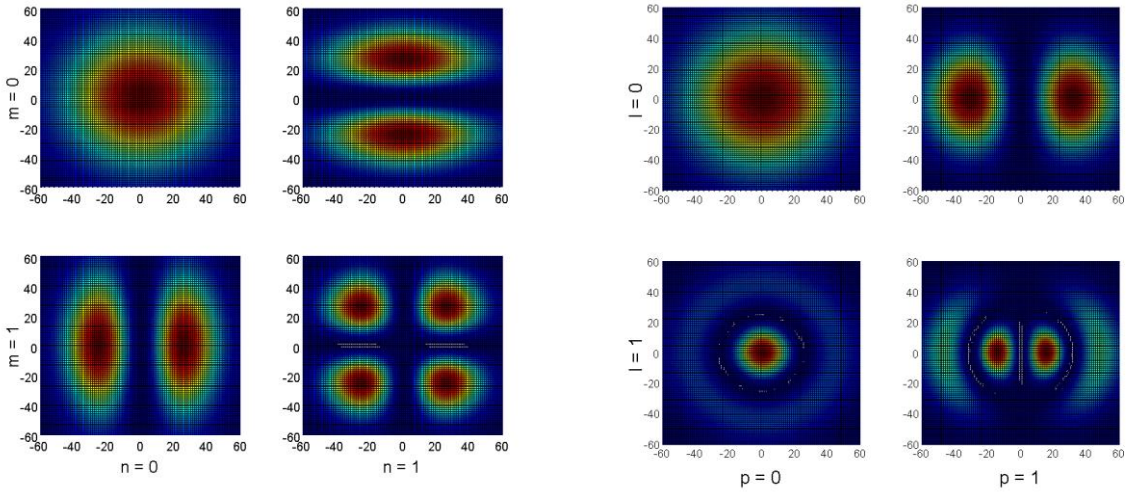

Figure 2.2 Intensity profiles of a square waveguide (left) and circular waveguide (right) for the lowest ordered modes. In the images m,n,l and p correspond to the indices given in Eqs. 2.3 and 2.4

2.2 Optical fibers

Optical fibers guide light through *T*otal *I*nternal *R*eflection (TIR). An optical fiber consists of the optically dense and in the case of fiber lasers, doped, core and the less dense and undoped cladding. Light traveling in an optically dense medium hitting the interface of an optically less dense medium at an angle below the critical angle will be completely reflected.[5] Often so called double clad (DC) fibers are used that consists of two separate claddings with different index of refraction, more on these later.

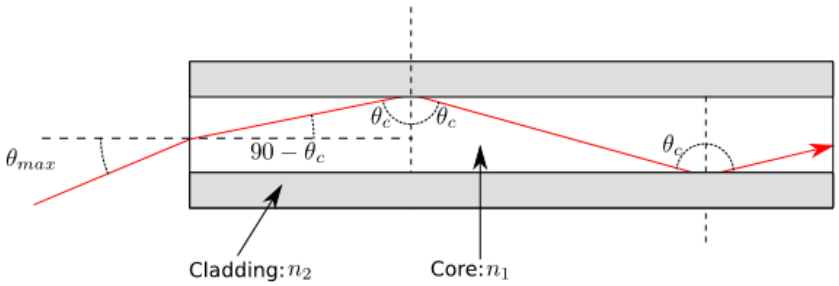

Figure 2.3 The defining geometry for the numerical aperture of an optical fiber. . [Image: "Fiber NA" licensed under Creative Commons CC0 1.0]

The square root of the difference in refractive index between core and cladding is called the Numerical Aperture, $NA = \sqrt{{n_1}^2 - {n_2}^2} = \sin\theta_{max}$ and, as can be seen in Fig. 2.3 defines the limiting maximum angle for incident light that is confined to the core. This means that a fiber with small NA will only guide light incident nearly normal to the fiber end surface and high NA will guide light at very large acceptance angles, increasing its light gathering capabilities.

A parameter related to the number of modes in a step index fiber is the normalized frequency or V-number defined as

$$V_{nr} = \frac{2\pi a}{\lambda} NA, \tag{2.5}$$

where *a* is core radius and λ is the wavelength of light in the core. For step index fibers a V-number below 2.405 ensures single transverse mode operation. Normally it is of interest to maximize pump light in the doped core. Therefore, since the pump beam quality is generally of lower quality than that of the output in a precision laser, a high NA is desirable to capture as much pump energy as possible while it is still important to retain a low enough core radius to ensure single mode operation. A balance between NA and core size is application dependent but it is important to realise they are trade-offs to each other if the goal is to retain single mode operation. This has led, among other solutions, to the development of DC fibers.

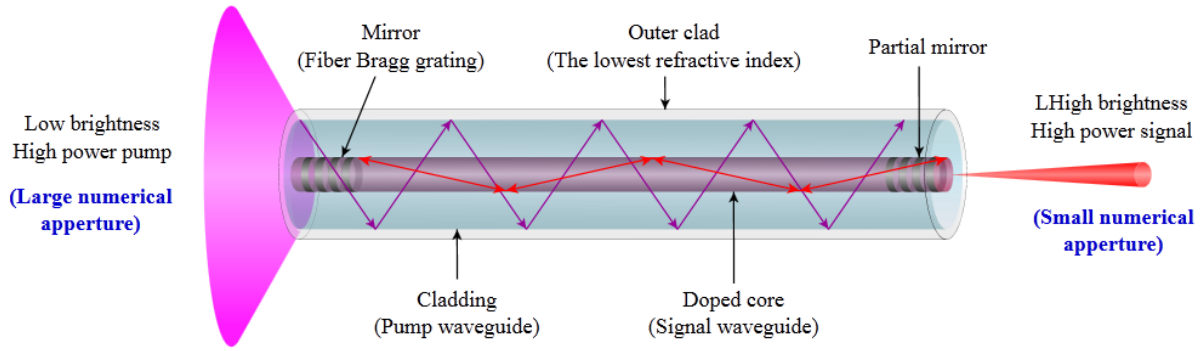

Figure 2.4 An example of a common use of DC fibers. From the left a beam from a high NA pump source is incident on the fiber and allowed to propagate through both core and cladding. FBGs are used to create an oscillator in the doped core to which the signal is confined. The emitted laser light has a much lower NA. [Image: "Schematic diagram of high power fiber laser using a double-clad fiber" licensed under Creative Commons CC0 1.0]

A DC fiber has a second cladding region between core and outer cladding of a differing refractive index yielding a difference in NA between outer-inner cladding and inner cladding and core.

The DC configuration of fibers significantly reduces the demands on the pump and facilitates the technique of cladding pumping fibers having a core doped with certain rare-earth metals. This method lets a high power, high NA pump propagate through the cladding and be gradually absorbed by the doped core. The laser light, or signal, will be confined to the core and keep the desired beam quality. The main drawback of this pumping method is that the main power of the pump will at any given time mainly propagate through the cladding, meaning that much longer fibers are required for the pump light to be completely absorbed. A typical use of DC fiber can be seen in Fig. 2.4.

A key parameter in guided propagation is the beam propagation constant, or commonly β in literature. It is defined as

$$\beta = n_i k \cdot sin(\theta) \tag{2.6}$$

Here n_i is the index of the medium in which light propagates, k is the vacuum wave vector and the angle θ is the angle between k and a vertical line perpendicular to the beam propagation axis (in 2D), i.e β is the projection of a phase front in the direction of the propagation axis. Furthermore, since transverse modes are at a slight angle to the propagation axis, β can be considered a modal index.

The effective mode index $n_{eff}(\lambda, n)$ is a number quantifying the phase delay per unit length in a waveguide, relative to the phase delay in vacuum and is related to the beam propagation constant β as

$$\frac{\beta}{k} = n_{eff}. \tag{2.7}$$

Effective index is therefore an inherent material property and is both wavelength and mode dependent, it is a key parameter in guided propagation, just as refractive index is to unguided propagation and it is an especially important factor in fiber optics. Since fiber geometry is easily manipulated and effective index is an inherently geometric property, effective index can to some extent be controlled by manipulation of the fiber [6].

2.3 Mode improvement using fiber coiling

Another method to improve the beam quality, particularly in fibers with larger core radius, in which many transverse modes are allowed, is the practice of fiber coiling. The basis for this method is the fact that the effective refractive index differ for different transverse modes[6]. When the fiber is bent there is an induced slope in the effective refractive index profile which narrows the refractive index barrier on one side of the slope. Since the effective refractive index is lower for higher order modes there is a curvature radius range where the barrier is narrow enough to allow the higher order modes to tunnel into the cladding (Fig 2.5) making them have a much higher loss than the fundamental mode [7]. Using this technique, it is possible to scale up to much higher core sizes, into the 20-30µm range, and still keep single or near single mode operation. Another benefit of this is that the pump absorption scales quadratically with the core size for a given inner cladding diameter permitting the use of shorter fibers. Alternately increasing the size of both the core and the inner cladding permits the use of much stronger pump sources.

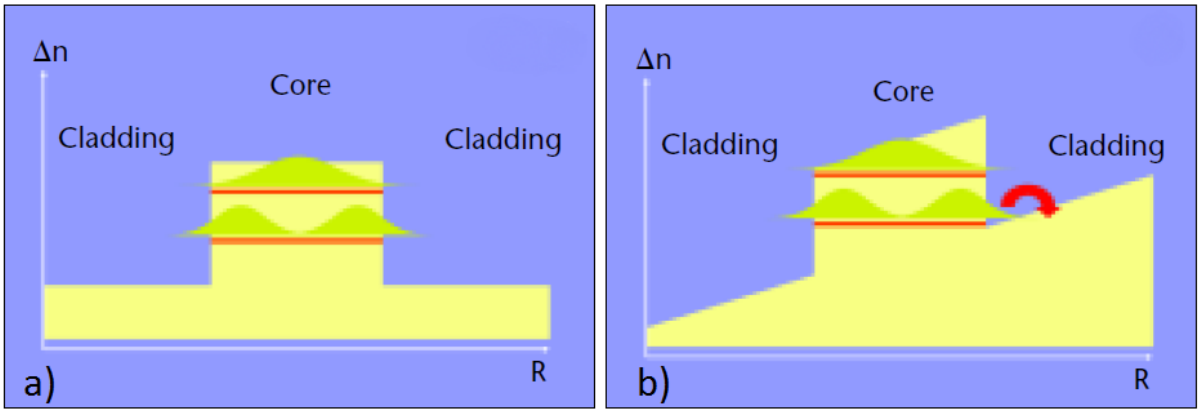

Figure 2.5 show schematic views of the effective refractive index in an optical fiber. a) An uncoiled fiber. Both the fundamental mode and higher order modes are confined to the core. The higher ordered modes experiences a lower effective index [Δn] but the barrier between core and cladding is still large enough to contain them. b) A coiled or bent fiber. By coiling the fiber around a cylinder it is possible to induce a shift in effective index. Effectively the potential barrier between core and cladding is lowered permitting higher ordered modes confined to the core to tunnel into the cladding.

2.4 Fiber Gratings

A common way of affecting light in fibers is by the use of periodically shifting refractive indexes along the core, effectively creating an optical grating along the direction of the beam propagation axis. These shifts are accomplished by e.g. submitting photosensitive fiber to an interference pattern from a UV laser source, creating an extremely wavelength selective structure [8] called Fiber Bragg Gratings (FBGs).

Gratings have many uses, including but not limited to band filtering, dispersion compensation and in-fiber sensing. It is also possible to use FBGs as highly wavelength selective mirrors. These can be used as in-fiber high and low reflectors to create a cavity containing a doped fiber.

A uniform Bragg grating is a grating where both refractive index change δn and grating period Λ are constant over the whole grating length. There are several other shapes and sizes of gratings with different properties but it is instructive to look at uniform gratings since it makes the equations easier and serves to clearly show some of the different aspects to keep in mind while designing or choosing FBGs as well as being directly applicable to the gratings used and evaluated later.

The starting point of any reflective grating is the reflected wavelength. A mode incident on the grating of a certain period Λ, which is reflected as an identical but counter-propagating mode fulfils the familiar Bragg condition:

$$\lambda_{Bragg} = 2n_{eff}\,\Lambda, \tag{2.8}$$

Λ is limited by fiber properties such as doping and the precision of the equipment used in its creation. With Ω being the coupling coefficient between modes for a sinusoidal core refractive index variation, $\eta(V) = 1 - \frac{1}{V^2}$ expressing the fraction of power in the core (*V* is the V number from Eq. 2.5), $\Delta k = \beta - \frac{\pi}{\Lambda}$ being detuning wave vector, $s = \sqrt{\Omega^2 - \Delta k^2}$ and *L* grating length. The term δn is called index modulation and is a measure of the relative shift in refractive index from the core index [9]. Using coupled mode theory to solve several mode specific differential equations the reflectivity of a specific grating can be expressed as [9]:

$$R(L,\lambda) = \frac{\Omega^2 sinh^2(sL)}{\Delta k^2 sinh^2(sL) + s^2 cosh^2(sL)} \tag{2.9}$$

$$\Omega = \frac{\pi \delta n \eta(V)}{\lambda} \tag{2.10}$$

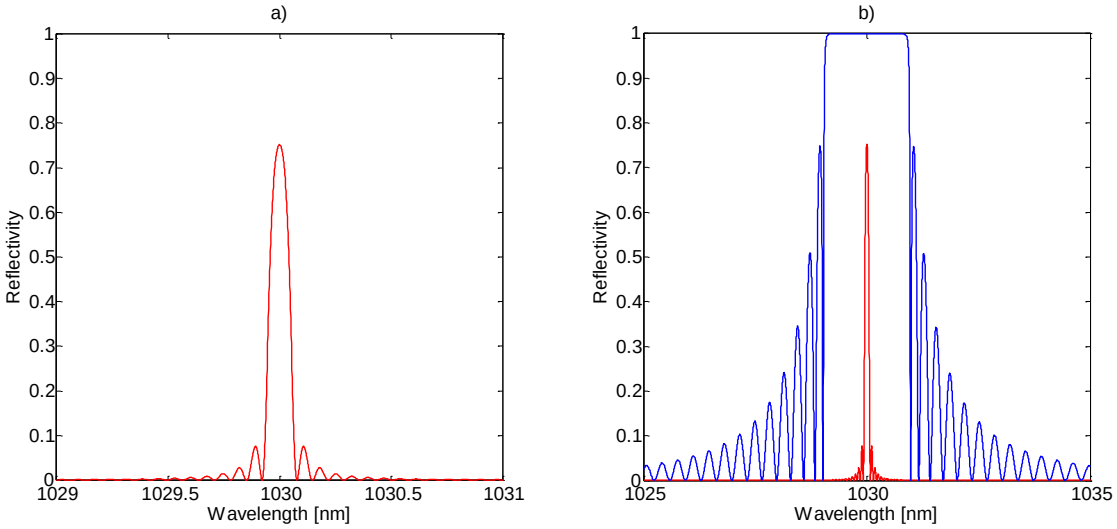

Figure 2.6: Simulation of two different gratings centred at 1030nm with different grating lengths and refractive index modulations. Grating A (left) is 5 mm long and has an index modulation δn of 10^{-4}. Grating B (right, with A as reference) is 1mm long and has an index modulation δn of $3 \cdot 10^{-3}$. The result is a significant difference in reflective properties and bandwidth.

Two gratings are simulated and compared in Fig. 2.6. The Full Bandwidth, or the zero-to-zero bandwidth, is defined as the bandwidth between the first zeroes and given by:

$$\Delta\lambda_{FB} \cong \frac{\lambda_{Bragg}^2}{n_{eff}\,\pi L}[(\Omega L)^2 + \pi^2]^{\frac{1}{2}}. \qquad (2.11)$$

Together with the equations 2.8-2.10 this facilitates a very rudimentary estimation of important grating properties. For example it is of prime interest to look at reflectivity and bandwidth since these factors define two of the most important properties at a given wavelength. These factors at different values δn are shown at a central wavelength of 1030 nm in Fig. 2.7.

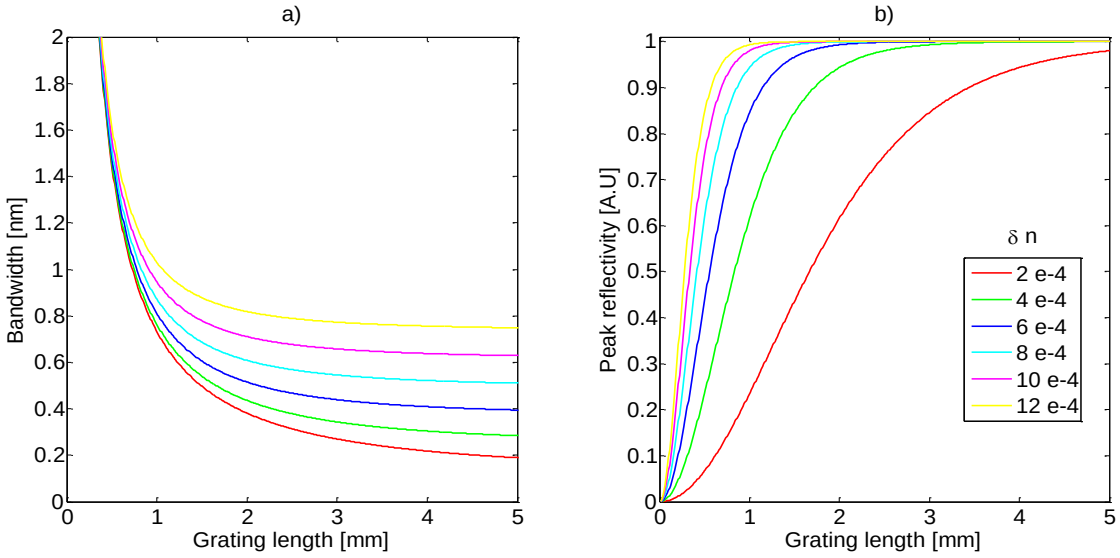

Figure 2.7: Bandwidth (a) and reflectivity (b) as function of grating length for different values of refractive index change δn.

2.5 Ytterbium

There are several available lanthanide dopants available when choosing what kind of system to build. Among the more common ones are Erbium, Ytterbium and Neodymium. Among the less common are Dysprosium, Praseodymium and Thulium. Several different aspects need to be evaluated when deciding upon a particular one to use in experiments. The foremost consideration of which are the emission wavelengths of the dopant in silica fiber as well as the sensitivity of available detectors at these wavelengths. All of the above dopants could be used to build a laser, especially Praseodymium since the possibility to build a visible light source would be ideal to maintain a high sensitivity in the current detector. This would also eliminate any need to use frequency doubling on a far infrared source. However, Praseodymium is not a very common dopant compared to for example Erbium or Ytterbium. The rise of fiber communication over the past years has made Erbium a common dopant and a lot of the research around Erbium has analogues in Ytterbium. Equipment used in manufacturing is developed. Various optical fibers for use with these particular dopants are readily available, and lead times are low for both. Ytterbium however, emits light at wavelengths lower than the common Erbium emission around 1.55µm. The detectors used by LTH have a much higher sensitivity at wavelengths around 1µm and therefore Ytterbium is the better choice in a fiber-laser scenario.

Ytterbium is an increasingly popular dopant for high power fiber applications [10, 11]. As depicted in Fig 2.8 all laser action in Ytterbium relies on the two stark-split manifolds $^2F_{5/2}$ and $^2F_{7/2}$. One attractive aspect of these transitions is its high slope efficiency, the material intrinsic ratio of output power versus pump power. This is partly because of the lack of Excited State Absorption (ESA), a phenomenon where electrons or ions in an already excited state absorb laser level photons. This is impossible in Ytterbium since it relies on transitions from ground state to different stark levels rather than transitions between multiple electronic levels. Another positive aspect is again due to its many and narrowly spaced stark levels. These give rise to an extended and almost continuous absorption band stretching from 850nm to 1070nm [10]. Likewise emission is equally semi-continuous and ranges from 940nm to 1200nm. Both the absorption and emission spectrum is shown in Fig. 2.9.

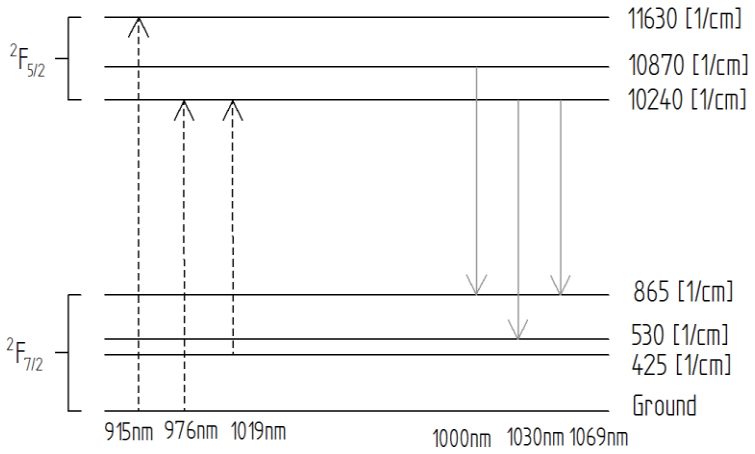

Figure 2.8: Stark levels of Ytterbium.

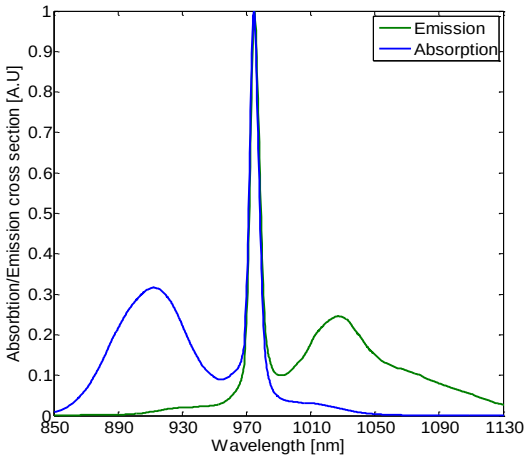

Figure 2.9: Absorption and Emission cross sections of Ytterbium.

2.6 Holography

Holography is a technique enabling three dimensional imaging of objects. The basic method of holography uses narrow bandwidth laser light split into an object beam and a reference beam. After recombination the resulting interference pattern is recorded on to a medium, such as a holographic plate, similar to a photographic film, or by a digital camera.

One example of a multi wavelength interferometry setup [12] called an equal path interferometer is used for measuring the flatness of surfaces. This type of setup is shown in Figure 2.10 and bears special relevance since a variation on this is planned to be used in conjunction with the laser from this work.

As can be seen in Fig. 2.10 the laser beam is first split into two separate beams of light.

The object beam is made to illuminate the object that is to be recorded as a hologram and reflected onto the recording medium. According to diffraction theory [5] each point of the object that reflects light can be considered a point source that illuminates the medium.

The reference beam is made to pass space undisturbed to illuminate the recording medium directly and therefore contains the original beam phase information.

Each point source from the object individually interferes with the reference beam resulting in the pattern of a sinusoidal zone plate [5]. These patterns combine to create a complex speckle pattern on the recording medium, and in the case of a holographic plate, contain all the phase information of the point sources.

When the holographic plate is later illuminated by a beam identical to the original reference beam each of the zone plates recreate the phase information of the object wave that created it and combine to create a virtual image of the original object.

As discussed in the introduction, a problem when performing *digital* holographic metrology is the existence of a 2π phase ambiguity between the reference and the object beam which require prior knowledge of the approximate distance being measured with sub wavelength accuracy to resolve. Due to the periodic nature of the electromagnetic field, resolution of phase difference in interferometry is limited to a 2π interval. Phase differences outside of the 2π range are wrapped back into this interval, i.e. it is impossible to distinguish between π and 3π phase difference resulting in an unambiguous measuring length of half the measuring wavelength ($\lambda/2$) [1] . The phase difference between two interferometer phases, obtained from measurements at different wavelengths act like a single phase with a corresponding synthetic wavelength longer than the individual wavelengths used [1]. Using several synthetic wavelengths and repeating the process it is possible to effectively synthesize even longer unambiguous lengths, enabling measurements of much larger lengths or depths.[1-3]. The synthetic wavelength is defined as

$$\Lambda_{ij} = \frac{\lambda_i \lambda_j}{\lambda_j - \lambda_i} \tag{2.12}$$

Where λ_i and λ_j are the actual wavelengths used for the interferometric measurements.

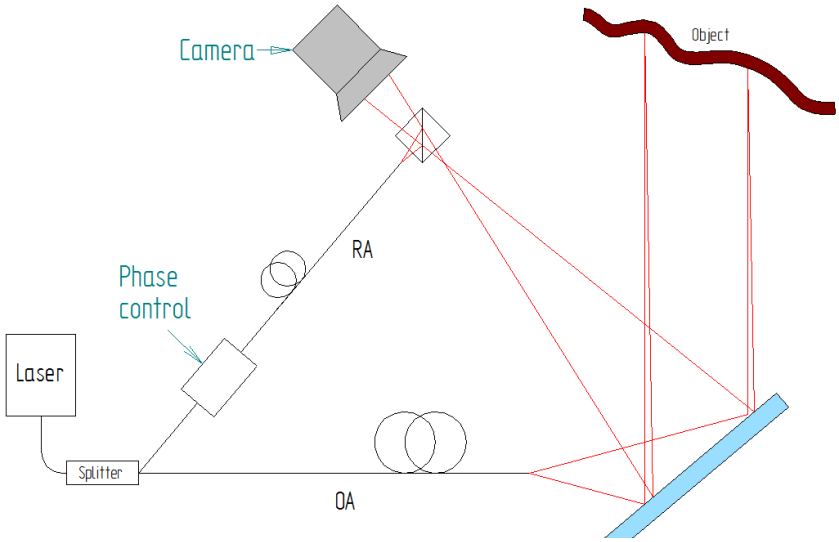

Figure 2.10: Equal path interferometer. Light from the object arm OA, and the reference arm RA are recombined after separate paths and recorded wwith a suitable detector.

Using the information from several different measurements, it is possible to digitally recreate the surface using Fourier transform [13].

3 Evaluation work

In a first effort to find a suitable system for a prototype, several theoretical systems were created and discussed. The systems were all evaluated regarding expected construction time and complexity, industrial viability, approximate costs involved, scalability, and of course, expected performance. Several more or less outlandish ideas were discussed and yet other potential solutions were deemed to take far too long to complete or be far too complex for the span of this master thesis project.

The ideal demands on the system are reiterated for the reader's convenience.

". Firstly the laser should be as simple as possible, meaning it should be potentially cheap to build in larger volumes. Second, it should be transverse and longitudinally single mode. Furthermore it would be ideal if it was possible to scale the system to deliver 10 to 15 separate wavelengths spectrally separated by 1nm. It should be possible to synchronically pulse the lasers in 1µs pulses with about 0.1mJ pulse energy per wavelength. Lastly the light should be visible or near infrared wavelengths to facilitate the use of common commercial detectors."

For the sake of brevity only the more realistic setups are presented here to give the reader some appreciation of the ideas that were involved in the decision making process.

3.1 Two or more diode lasers with bundled fiber pigtails, fiber Bragg gratings and common collimator.

A first preliminary idea discussed was the use of several fiber pigtailed diode lasers, each of the pigtail fibers would contain a fiber Bragg grating to lock each diode to a specific wavelength. The fibers would then be bundled using a silica capillary (or glue if one is so inclined) and collimated using a common collimating lens.

While being one of the simpler solutions this particular setup fails to deliver anything but the demands (Sec 3.0) on transversal single mode and single frequency. Scalability is very straightforward by just adding more diodes. Another advantage is the possible use of visible light wavelengths; something that is common and inexpensive compared to for example IR diodes. While it would be possible to put the diodes on the same driver and temperature controller , effectively reducing the system total cost, it would introduce a problem with the lasers not delivering at equal powers, or at the least reduce the ability to manipulate power discrepancies without shifting the wavelengths thus limiting control over for example drifting.

The main issue with this solution is that it merely allows for testing and the possibility to confirm and showcase the use of method for 3D imaging, not creating a platform for future development of a perfectible system.

An alternative to the bundled pigtails can be seen in Fig.3.1 which shows a diode laser array external cavity setup to both combine the beams and force the operation at different wavelengths of different array elements using a transform lens, a grating and a common output coupler [14].

Yet another alternative building upon the idea of using arrays is to use a diode laser array with the lasers locked to single frequency by use of a chirped volume Bragg grating after the array and focus work on free space beam combining.

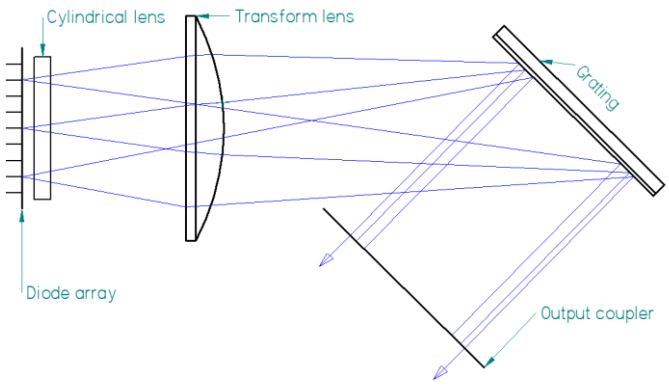

Figure 3.1: Light from a diode laser array is collected using a pair of lenses and projected on to a diffraction grating. The individual lasers in the array are stabilized at selected wavelengths using the first order reflection from the grating

3.2 Free single mode diode lasers with common ytterbium fiber amplifier.

Fig 3.2 shows how several diode lasers are locked to different wavelengths by use of FBGs . Using a mirror or system of mirrors the seeds are free space coupled into a several meters long Ytterbium-doped fiber for amplification. This fiber is pumped from the other end by another laser at the common 915nm or 976nm wavelengths [10]. Seed and pump would be separated by a dichroic mirror.

The size of this amplification fiber is limited by the need to keep a TEM_{00} profile and how much can be compensated by fiber coiling and other techniques. The choice of Ytterbium is due to its good availability, wealth of research on Yb-amplification and that it is closer to the lower IR-band than for example Erbium. A system with amplified diode lasers would be closer to the specifications (Sec 3.0) on output power than the laser described in the previous section 3.1. Ideally it would generate ~2W per wavelength CW or QCW depending on pump power and the number of seeds, and have the advantage that adding another seed would be comparatively easy. However, a severe limitation when more seeds are added would be that all they would all share the same amplification setup giving more wavelengths at the expense of individual output power.

Another problem with this solution is that laser diodes at wavelengths around 1030 is comparatively uncommon and therefore suffer from high pricing and long lead times. The problem with multiple individually driven and temperature controlled parts persist with the added problem of different amplification at different wavelengths.

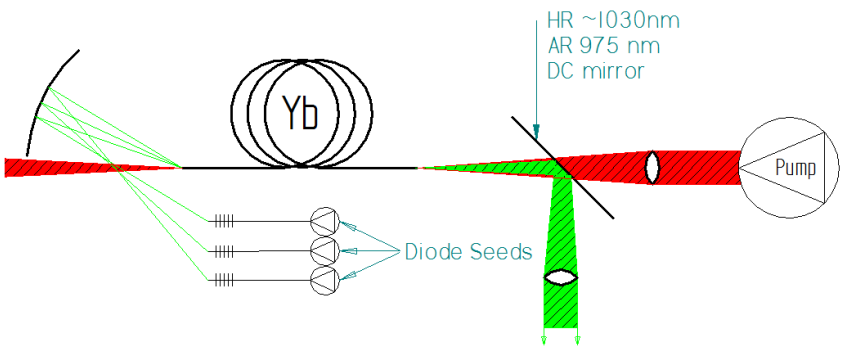

Figure 3.2: Seed lasers and pump laser coupled into Yb-fiber from different directions to easily separate the different signals from each other. Separation is accomplished using a dichroic (DC) mirror with high reflectance (HR) properties for the seed wavelengths and anti-reflectance (AR) coating suited for the pump wavelength.

3.3 All fiber, branched fiber lasers with separate amplification and single pump.

A very elegant and robust solution depicted in Fig. 3.3 would be to fuse a single pump source to a collection of capillary bundled fibers. These would function as a splitter for several pump delivery fibers leading to separate wavelength-locked ytterbium doped cavities using FBGs as end mirrors. These are in turn fused on to longer Ytterbium-doped fiber amplifiers. An all fiber or almost all fiber solution has many advantages over free space solutions as pertaining to the end user.

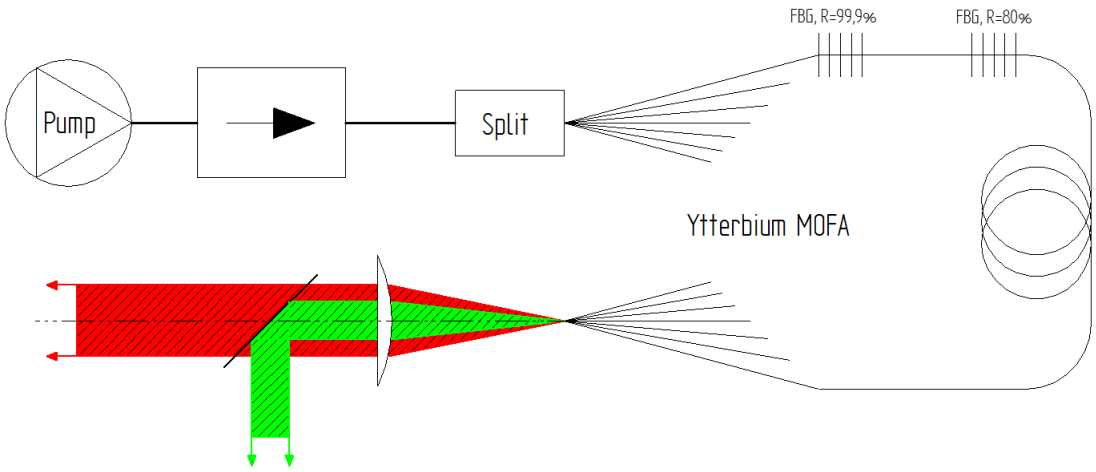

Figure 3.3: An all fiber solution. Pump light is split in to several pump delivery fibers and used to drive several fiber lasers. The fiber lasers are constructed using both high (R=99.9%) and low (R=80%) reflectance FBGs. Each laser is spliced on to a master oscillation fiber amplifier (MOFA). After common collimation seed and pump are separated by a dichroic mirror.

For example it is possible to take advantage of the characteristic fiber strengths such as high beam quality, long coherence lengths, compactness, and insensitivity to mechanical disturbances and pollution compared to mirrors and other free space optical components. The thermal properties of lasers are of considerable import in high power setups and the use of fibers allows for good heat dissipation since fibers have low volume to area ratios. They are also easily cooled using for example, water baths, due to the fact that they can be completely submerged without adversely affecting function. The fact that it uses a single pump source makes it cheaper and in theory easier to service and maintain. This type of construction could be made using modular parts increasing ease of maintenance and part replacement further.

While very attractive on paper a system like this suffers from a number of difficulties. The individual amplified powers will in all probability not be very high in a thin ~6 µm fiber compared to what could be achieved using larger core non single mode fibers. It is also easy to imagine large losses of pump power if one of the many and sensitive components or splices

are faulty. Many of the proposed techniques used in the assembly are new, advanced and/or untried. For example, the idea of using a capillary bundled fusion spliced split is not extensively tried or researched and above all not something that is readily commercially available. Pulsing is in the scope of this Master thesis project limited to electrical pulsing of the pump diode. If done industrially pulsing would probably be done by piezo elements on the individual cavities. This could possibly affect the otherwise high robustness of the setup adversely.

While it is hard to guess the actual output powers and the characteristics for the long term, this solution still has some very interesting opportunities for further development. Areas such as the balance between pulse powers, beam quality, pump power, fiber size, cooling, split power handling, pulsing techniques, modularity and robustness promise groundwork for long and interesting further development process possibly spanning years.

3.4 Q-switched, flash lamp pumped, common cavity mini lasers with VBG beam combining.

Building upon earlier experiments and experience at KTH it might be possible to adapt an already constructed flash lamp pumped laser to single frequency using volume Bragg gratings, VBGs. The idea would be to use VBGs to achieve good beam combination and using an active or passive Q-switch, common for all lasers, for pulsing. Fig. 3.4 shows an example of such a setup.

It is the only of the proposed solutions that guarantees to match the proposed demands on output power. The existing model is capable of delivering 1J pulses at 0,2Hz and should be possible to modify to deliver 10mJ, 10Hz very short pulses in the order of 30ns. It is also very cheap and small considering its power.

The work in this case would focus on using VBGs to lock the wavelengths and to simultaneously combine the beams of several lasers. The pumping scheme would need to be modified with additional evenly distributed flash lamps to produce a more uniform illumination thus improving beam quality. This model might need the incorporation of a good liquid cooling system since the amount of heat generated by a 10mJ flash lamp laser is considerable.

One of the biggest disadvantages in this case is the issue with flash lamp lifetime. This number is hard to predict but it is believed that a laser generating 100mJ pulses could generate approximately 10 000 pulses. This however is very system dependent and hard to predict. Commercially available alternatives deliver anything from 10 000 to 100 000 000 pulses. Actual numbers on a working prototype would need to be examined but it is easy to see that a system delivering 10 000 - 100 000 pulses would be a severe limiting factor in an industrial environment since it would force a change of lamps at very narrow intervals significantly increasing costs.

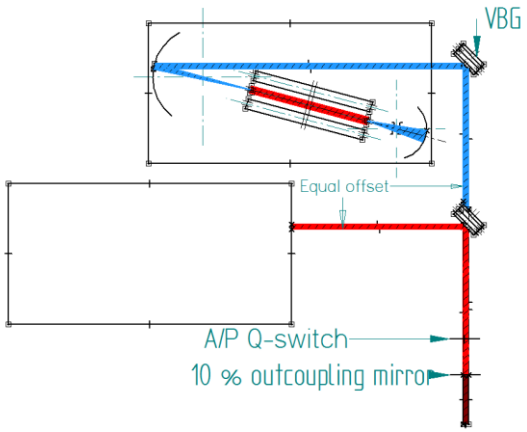

Figure 3.4: Several VBG stabilized and combined mini-lasers using a common active or passive (A/P) Q-switch. The offset between different laser housings is to ensure equal cavity length.

3.5 Diode pumped solid state lasers, DPSS lasers.

Also among the very robust and stable variants that could be built are the diode pumped solid state lasers. Included in this family are several conventional setups using different variants of end mirrors, VBGs, pumps, gain media and other components.

Of particular interest among the DPSS lasers are the family of Non Planar Ring Oscillators NPROs (or MISERS). Conceptually they differ little from ordinary linear DPSS cavities except that light incident on the NPRO makes semicircular roundtrips in the crystal. This special kind of laser consisting of a pump and a single ring cavity are very wavelength stable and, due to their short cavity size, can be made to work in single frequency. They are also fairly easily tunable, if one so wishes, using pressure induce birefringence. An NPRO both has a very high mechanical and thermal robustness making it suitable for continuous industrial work. [15, 16]

Being an integral part of NPRO design and function, using internal reflections, polarization can be achieved intra cavity without the use of other types of common polarization techniques. Another feature is that no external cavity mirrors or other components are needed other than cooling and pump making it possible to make an NPRO very compact indeed.

In this case, the main disadvantage would be the need for several individually pumped lasers. Add to this the fact that beam combining is not trivial, canceling any advantage in size it may have had without it, whereas fiber lasers can simply be bundled and still achieve expected results.

3.6 Vertical Cavity Surface Emitting Laser, VCSEL and Vertical External Cavity Surface Emitting Laser, VECSEL.

The V(E)CSEL which is depicted schematically in Fig 3.6 is a type of semiconductor laser consisting of a quantum well between two distributed Bragg mirrors. V(E)CSELs emit perpendicular from the top surface, as opposed to conventional diode lasers that emit from the cleaved end of a wafer. This allows for a perfect circular beam profile instead elliptical that is normally the case with diode lasers.

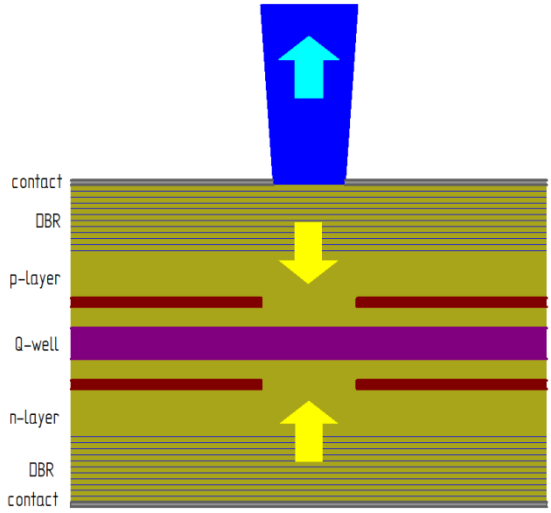

Figure 3.5: A typical VCSEL. A resonator is constructed between electrical contacts. The laser resonator consists of two distributed Bragg reflector (DBR) regions parallel to a semi conducting wafer surface with an active region consisting of a quantum well for laser light generation in between.

The VCSEL as well as the VECSEL both have attractive spectral properties; a very short cavity length ensures a large free spectral range making single mode operation easily achieved. The biggest drawback of the VCSEL is the limitation on the output power. Due to the extremely high reflectivities needed on the Bragg mirrors brought on by extremely short gain media, output powers are limited to approximately 6 milliwatts.

Chalmers University of Technology was prepared to supply the VCSEL array but output powers were considered too low to be of practical use. This variant however, spawned the idea for the possible use in another project based on the same laser holography and signal processing methods adapted for small area investigations with fiber mounted cameras.

The VECSEL differs from the VCSEL in that where the VCSEL has two distributed Bragg reflectors as mirrors the VECSEL replaces one with an external mirror and is most commonly optically pumped. This external mirror allows a significantly larger area to participate in light generation consequently yielding much higher powers, in some cases up to 500 milliwatts [17]. Another interesting feature is that an open cavity lends itself particularly well to manipulation of emitted light such as frequency doubling.

The VECSEL approach had to be discarded due to technical limitations. The potential need for work with microelectronic components was considered to advanced and time-consuming to make it viable within the limits of this project.

3.7 Passively Q-switched Fiber-bundle laser

It has been demonstrated [18] that it is possible to simultaneously pump 250 highly Nd-doped fibers and pulsing them using a Cr^{4+}:YAG crystal for common passive Q-switching. This setup delivered a total of 10mJ in 35ns pulses.

The original experiment uses a common end mirror for all fibers instead of the FBGs shown in Fig 3.7. It might be possible to replace the end mirror with individual fiber FBGs in an attempt to create a simultaneously pumped and pulsed multi wavelength laser system.

Here the work would mainly concentrate on getting equal and stable output for all wavelengths, working with Neodymium, Ytterbium or Erbium fibers. Another issue is that power would have to be significantly amplified, about 50 times, for this solution to be viable. Creating a setup that would amplify this output in an elegant and non-cumbersome way is of course not trivial.

If these things could be realised it would be a compact and elegant solution indeed the main drawback again being flash lamp pumping.

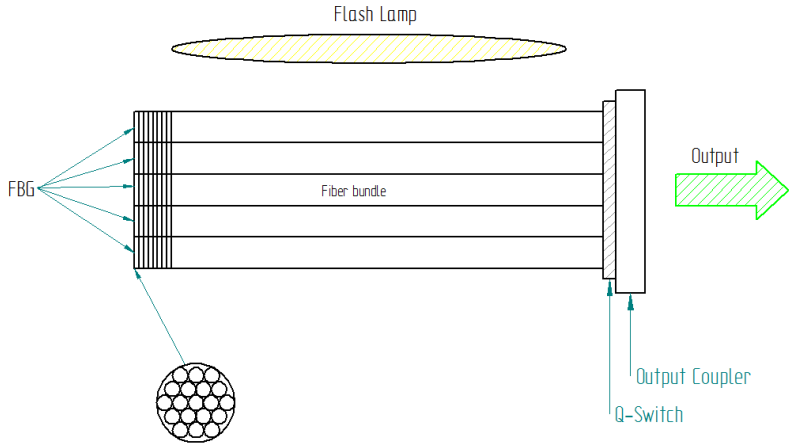

Figure 3.6: A bundle of fiber lasers. The resonators consists of doped fibers. In one end each has a FBG and in the other end all are fixed to a common Q-switch and output coupler (OC). The lasers are collectively pumped by one or more flash lamps.

4 The proposed solution

Although many of the proposed solutions would be possible it was generally considered that the variant with a single pump split into several fiber lasers with amplification (Sec. 3.3) was the most viable for construction and further study.

It had the many advantages of optical fibers such as heat dissipation, beam quality, compactness and power scaling as well as being fairly robust and possible to integrate in a demanding industrial environment where dust and vibrations are commonplace. Of course many prototypes could fit these criteria but the expected development cost of this particular variant was lower than many other, again making it a good canditdate for production.

Another aspect to consider was possible future development options. The fiber variant would be possible to scale in number of wavelengths. The pulsing could be developed using piezo elements and birefringence [19, 20] . Furthermore modularity, liquid cooling and power scaling as well as advanced variants of beam combining were considered attractive options and could eventually provide even further possibilities for various applications or refinement.

Although both variants using flash lamp pumping (Sects. 3.4 and 3.7) had individual qualities that made them attractive choices, the limits on flash lamp life times were considered too high to be economically and practically viable.

5 Laser development

5.1 Simulation

The starting point in deciding materials and techniques to be used was several rounds of simulations and discussions. Simulations were made with the help of software specifically designed to simulate Ytterbium fiber lasers. Also equipment specific software to simulate the writing of fiber gratings was used. The goal then, was to simulate a suitable geometrically compact narrow line-width laser, with FBGs as end mirrors to stabilize it. It was generally agreed that while shorter than 10 cm cavities could possibly be made, there would be a significant risk of damaging the gratings in the process, since there would be very small margins left in the splicing equipment to be used.

Our model was based on the use of Ytterbium doped DC fibers (LIEKKI™ Yb1200-6/125). These were readily available and were already used in several other experiments. This meant that all available equipment was able to handle these fibers hopefully preventing potential unforeseen setbacks. The particular LIEKKI™ fibers have a core NA of 0.15 a cladding NA of 0.46 and a peak cladding absorption of 2.6 dB/m at a pump wavelength of 976 nm. As a starting point 10 cm cavities were used.

The 6 µm core fibers are not theoretically single mode at the desired wavelengths around 1030 nm. Theoretical values for this fiber guarantees single mode operation only above 1178 nm. However, predictions were that this could be resolved by tight fiber coiling to couple out higher order modes from the fiber if necessary.

Simulations predicted that a laser lasing at just a few modes would be achievable using a 10 cm cavity and 60pm (zero to zero) bandwidth gratings as output couplers. These would give a maximum output power of the laser at 70-80% reflectivity.

Further simulations for the gratings confirmed that these theoretical values could be matched by available equipment for writing gratings.

5.2 Experimental setup

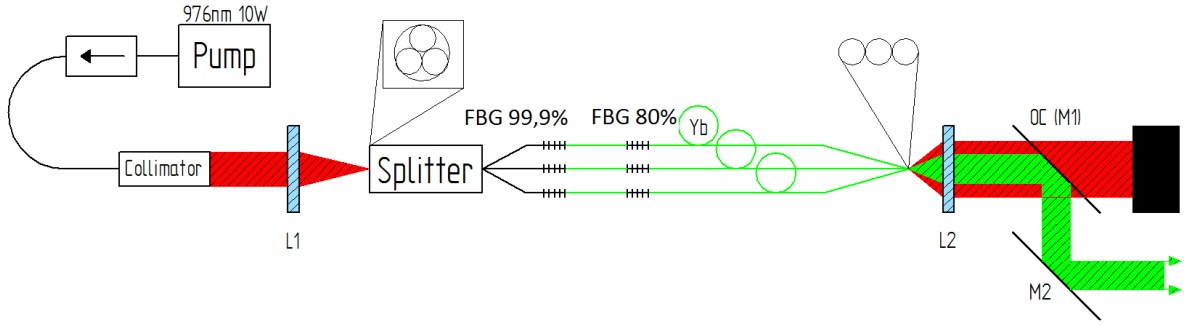

Figure 5.1: The final configuration of the lasers and connecting systems. L1 and L2 have f =15mm respectively 20mm aspheric and achromatic lenses. The output coupler (OC) M1 is a dichroic mirror that is high reflecting at 1030 nm and anti-reflecting at 976 nm.

The experimental setup is schematically illustrated in Fig.5.1. It shows a pump-laser simultaneously pumping three separate fiber lasers that are individually amplified. A single, feedback protected, fiber coupled diode laser emitting light at a wavelength of 976 nm was employed as the pump source. To achieve simultaneous and variable pumping of the three separate fiber lasers, the pump beam was coupled into a splitter by a collimator and lens L1 (f=15mm). The free space splitter enabled the arbitrary distribution of pump power into the three arms. Consequently, it was easy to test a single laser when needed or shift to simultaneous and equal output lasing power at other times. Each linear-structured laser consisted of a pair of fiber Bragg gratings and an 8 cm section of Yb-doped DC fiber (LIEKKI 6/125µm) resulting in 10 cm cavities. High-reflectivity gratings (R≈99,9%) spliced to the pump delivery arms of the splitter acted as a rear end mirrors while the relatively low reflecting gratings (R≈80%) acted as output couplers. Following the oscillator sections approximately 3m long amplifier sections were spliced using the same active Yb-doped DC fiber as for the oscillators. The amplified lasers were installed in parallel on a fiber holder, and collectively collimated using lens L2 (f=20mm). The dichroic mirror M1 separated the unabsorbed pump from the signal and the three signal outputs were monitored after mirror M2.

Fig 5.2 Shows the 3D modelling of the experimental setup. The model corresponds to the area between L1 and L2 in Fig. 5.1.

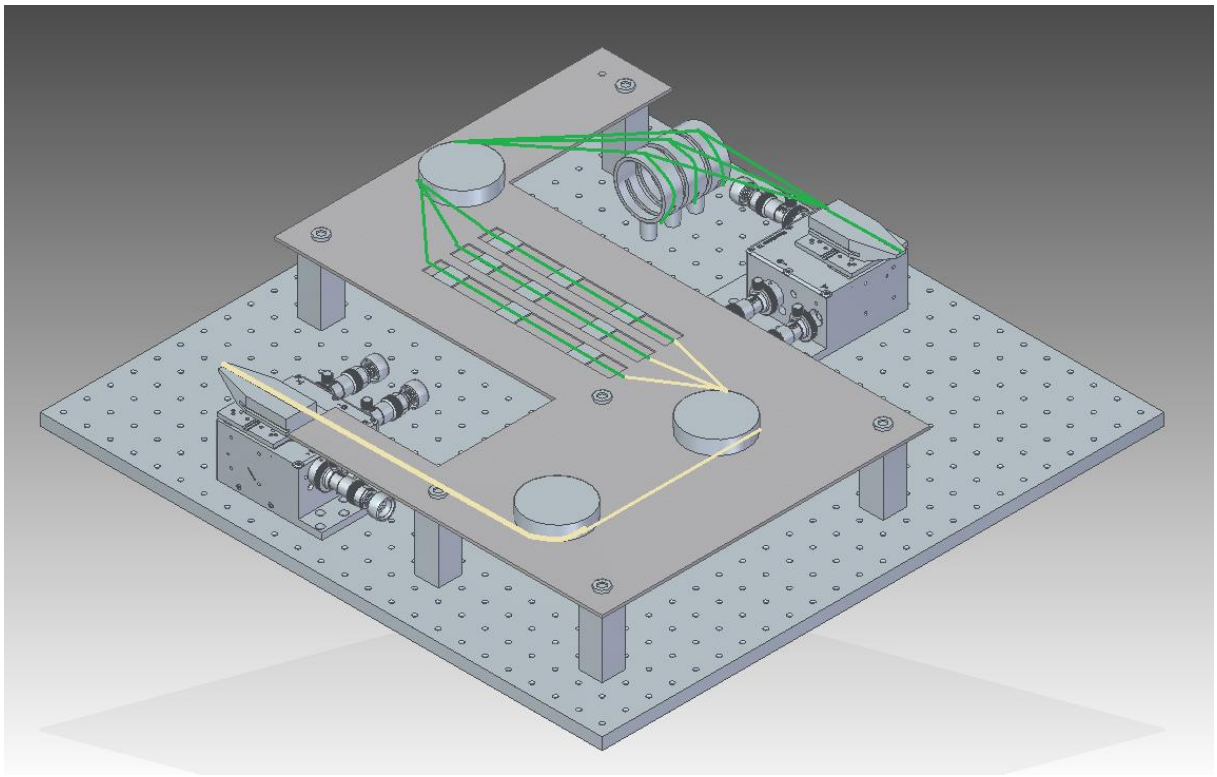

Figure 5.2. The custom made platform used to fix the lasers and amplifiers. Green lines symbolize active fibers and white is passive. The splitter is situated at the "lone end" of the white fiber.

5.2.1 Pump laser

The pump source employed in the experimental setup was a diode laser (JDSU-6398-L4ti) with a maximum output power of 10W. Driver, temperature controller and mount was an Arroyo Instruments 4320-QCW, a 5240 TEC source and an ARO-207, respectively, all of which are tailored to this particular line of JDSU diodes. The JDSU-6398-L4ti type of laser diode is specifically made for the pumping of Ytterbium doped fibers at 976nm. This particular laser is a fiber coupled diode laser with a fiber core diameter of 105µm and numerical aperture of 0.22. The pump laser also incorporates feedback protection at wavelengths between 1020-1100nm eliminating the need of e.g. a faraday isolator or other extra external components. The output was collimated using a fiber port collimator generating an output beam with a 3 mm beam waist.

Fig. 5.3 shows the pump laser spectrum at different drive currents and temperature. Note that the spectrum of the pump laser is fairly broad and uneven and as such it is hard to predict an optimal setting from data. Output wavelengths redshifts with both rising current and temperature, this is due to the band-gap in the active layer decreasing with increasing temperature (and active layer temperature increasing with the current). Maximum output power of the three fiber lasers was achieved by tuning pump temperature to 15 °C and drive current to around 11.5A yielding a somewhat unstable output power of 8W±15mW. This ensured pump operation at 976nm, or close to, given the broad spectrum of the pump source.

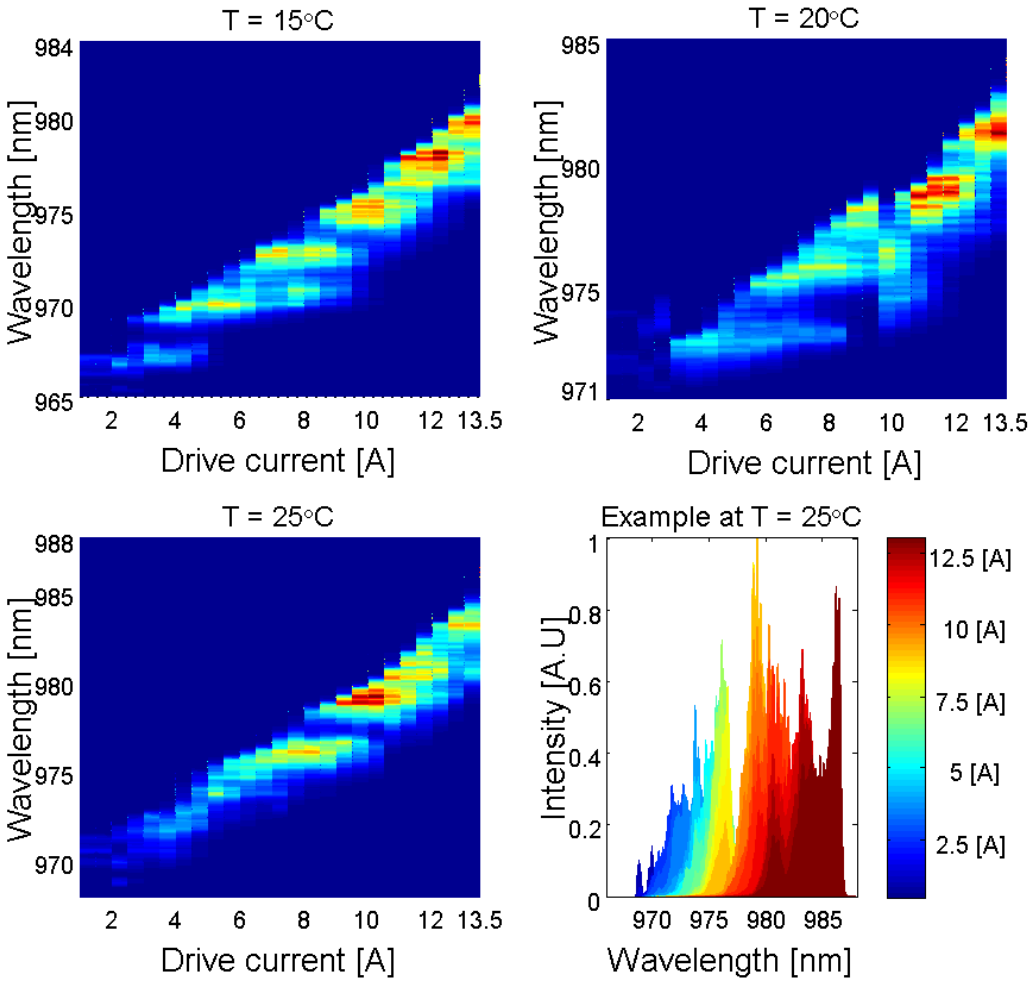

Figure 5.3. Topographical pictures of the relative pump powers of different wavelengths at different drive currents and temperatures. Lower right image shows the wavelength drift at different drive currents for a set temperature of 25°C .

5.2.2 Splitter

To ensure control over the output powers and the pump coupling as well as providing a high power alternative to commercial splitters, it was decided that an in house splitter should be constructed. This splitter was designed to facilitate easy variable- and simultaneous pumping of the three separate fiber lasers by letting the user manually control the input pump light into the splitter.

It was also a stated goal to create a type of component that might at some point be possible to splice directly onto a pump delivery fiber in an all fiber solution, given that equal power distribution without external control could be ensured. Several attempts had to be made to reach an acceptable end result, mostly since no predictions could be made and a trial and error approach had to be adopted.

The splitters were created by first taper down a ~1040 µm silica capillary to approximately 480µm using a glass fiber processing machine (Vytran GPX-3400), making it possible to hold three stripped 105µm fibers in an almost closed-packed fashion. The taper was done by heating the capillary and thinning it by slowly pulling at it. Three stripped fibers were inserted into the capillary after which it was further tapered around said fibers. The capillary holding the fiber bundle was then further down tapered to a desired dimension of 330 µm outer diameter. The capillary and fibers were then cleaved at the waist using a Vytran LDC-400 fiber cleaving machine in an effort to provide a flat end surface with three coalesced fibers.

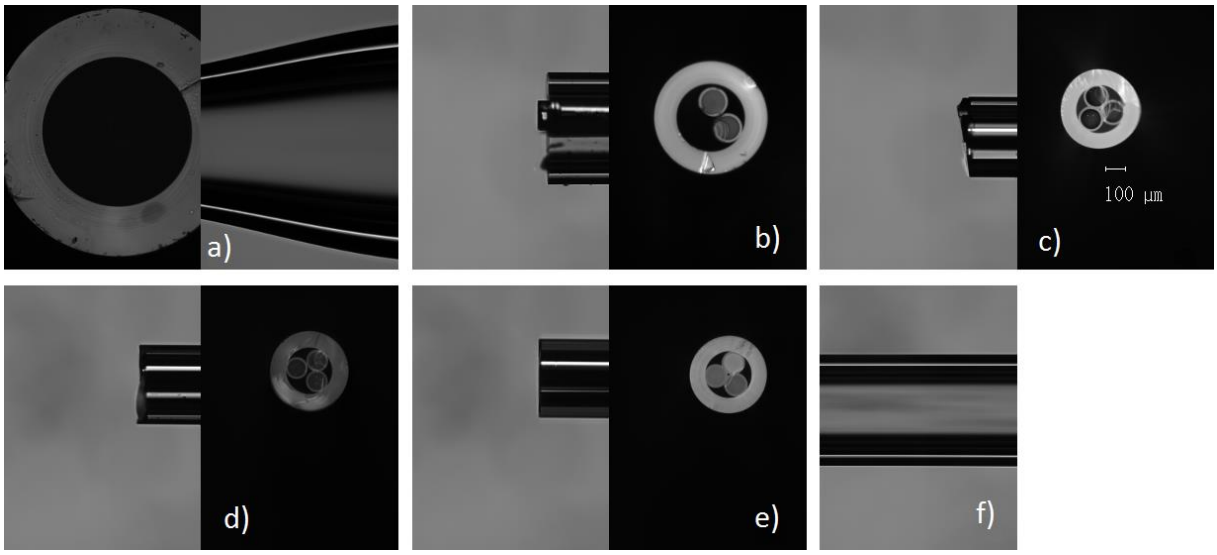

*Figure 5.4: Construction of the splitter. **A** shows the down tapered capillary before insertion of any fibers. **B-E** shows different results from the final cleave in chronological order, showing a "homing in" on correct settings on the fiber equipment. **F** show a side view of the capillary with 3 fibers inside.*

Fig. 5.4 shows some of the constructed splitters. While not perfect, the cleave on splitter e) was superior to the others, it was also the last one made. This was chosen to be used in the current setup. A fortunate side effect of using this particular splitter was an increase in coupling efficiency of the pump compared to coupling into a single fiber. While coupling the pump light into a 6/125µm passive fiber a coupling efficiency of 65% was achieved. In the case when the splitter was spliced into place

this number increased to a total of 74% when the three arms were calibrated to deliver equal output power.

5.2.3 Gratings

The fiber gratings needed to construct the fiber lasers were made using a 244nm argon laser in an interferometric setup (Fig 5.5). The gratings were written into the core of a passive single clad fiber (Thorlabs 1060 XP). While writing the gratings a Hamming apodization window function was used to

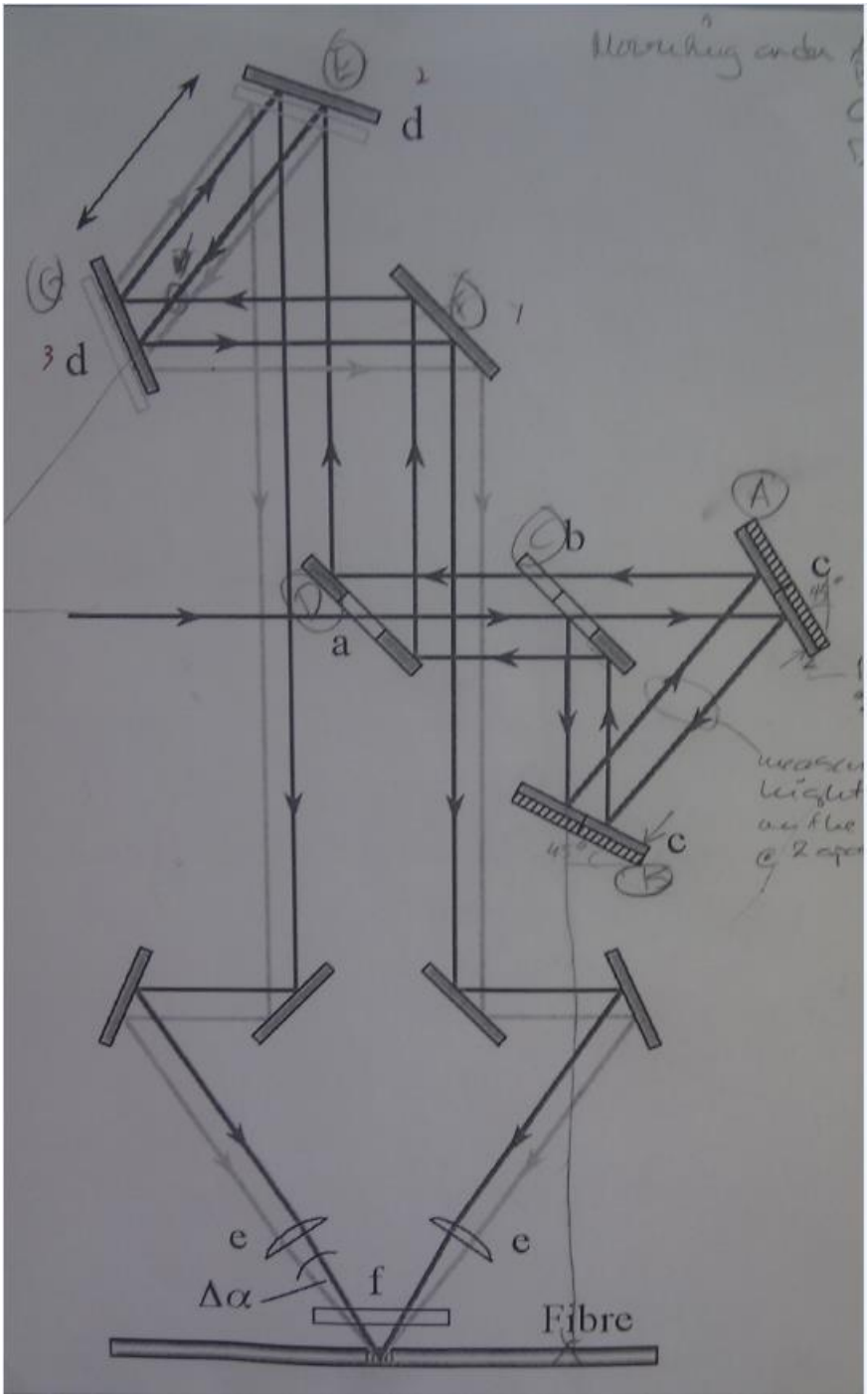

*Figure 5.5: Illustration of the interferometric setup used to write the gratings. Mirror system **a-d** can be shifted to change the incidence angle $\Delta\alpha$ after lenses **e**. Angle $\Delta\alpha$ decides the interference period and therefore grating period Λ.*

reduce side lobes [21]. Three high reflectivity (HR, R > 99%) gratings were needed as cavity end mirrors as well as three of slightly lower reflectivity (LR) around 80% were needed as output couplers. The HR gratings also needed to have a larger bandwidth than the LR to ensure the bandwidths matched both during normal operation and to compensate if there should occur slight thermal drifting of the central wavelength in one of the gratings.

Shown in Fig. 5.6 is an example of a typical end result when constructing the gratings, in this case with a reflectivity of 99.93% centred around 1029.212nm. Figure 5.7 presents a full list of the 17 gratings produced for this work. From these 17 gratings the six to be used as cavity mirrors were chosen according to matching bandwidths and reflectivities. Based on earlier simulations (ch. 5.1) it was decided to try to keep the output coupling gratings to around 80% reflectivity. The list of gratings in figure 5.9 allows for a rough ocular estimate for matching. The final stricter matching was done in Matlab using spectral information such as the one in Fig 5.9.

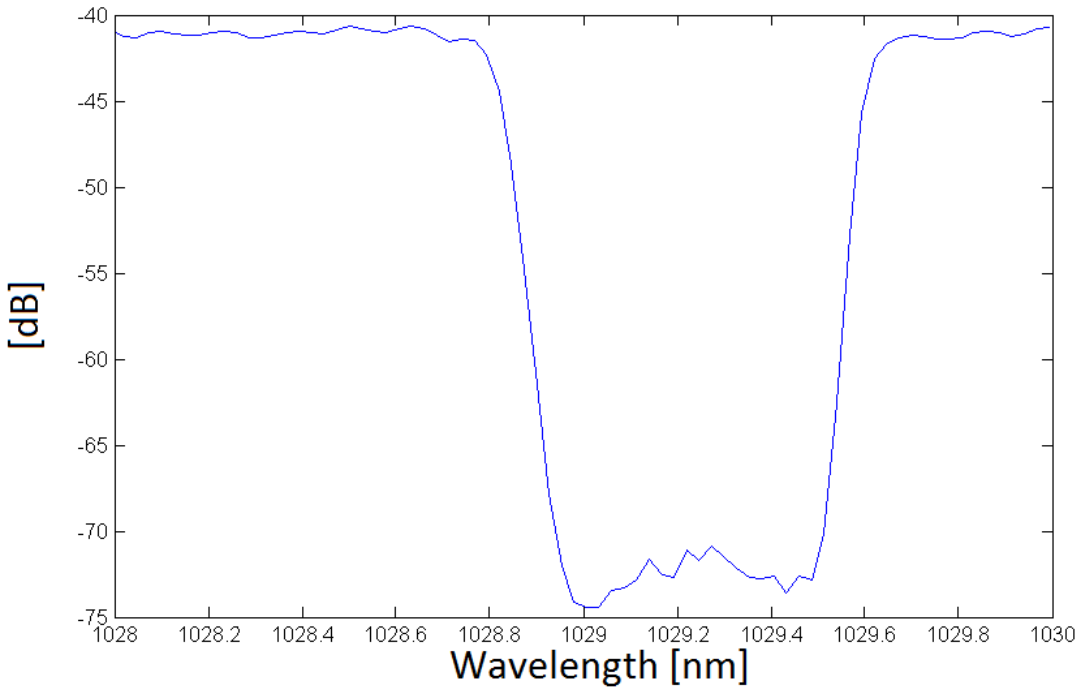

Figure 5.6: A typical high reflectivity grating. Central wavelength is around 1029.2 nm and the bandwidth is close to 0.8 nm.

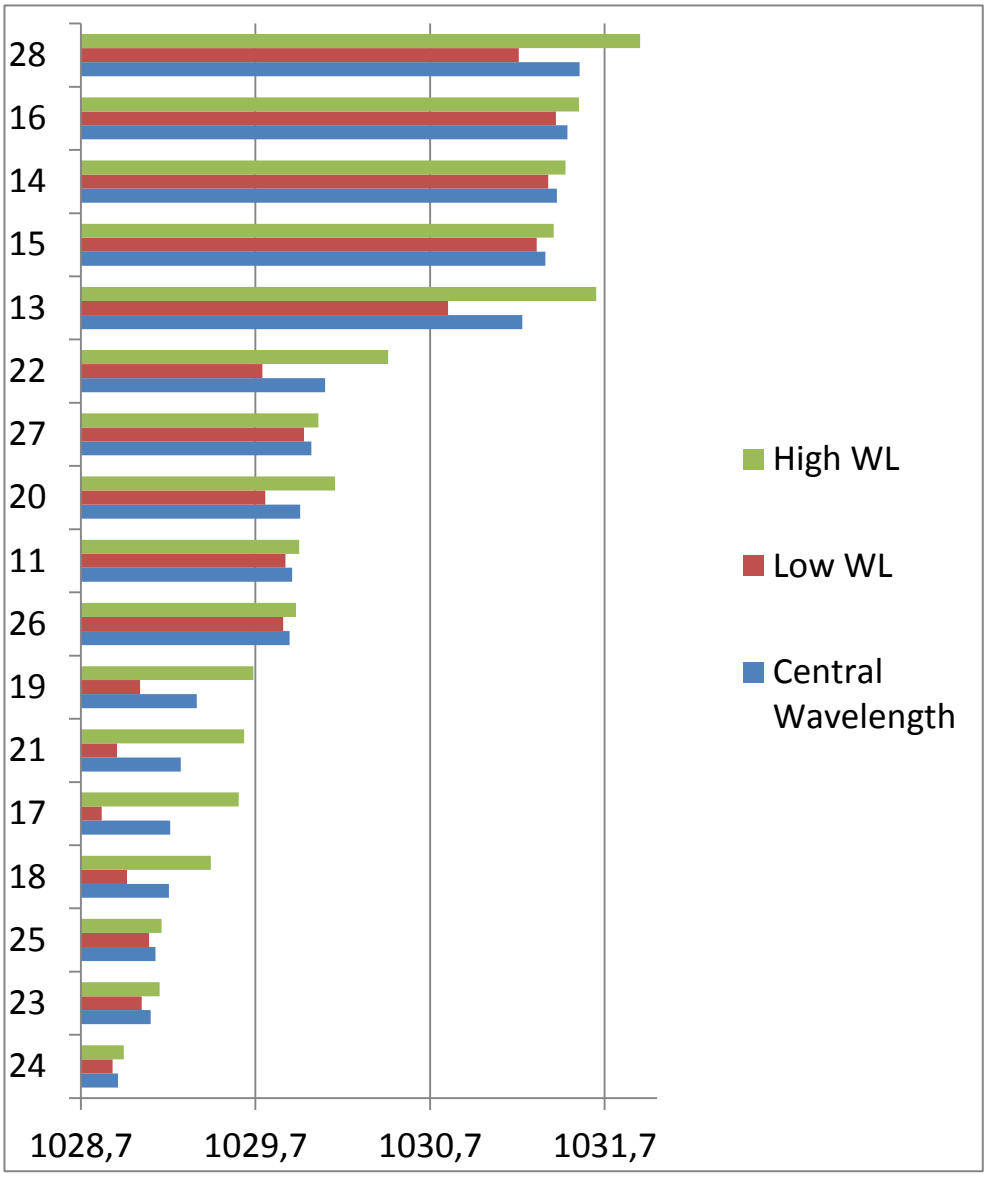

Figure 5.7: List of spectral properties of 17 gratings sorted by central wavelength. The list gives upper and lower spectral bounds of the gratings (or zero-zero bandwidth if one is so inclined), as well as central wavelength for quick and easy ocular comparison and matching. Numbering is for identification only.

5.2.4 Lasers

The fiber lasers were all constructed using gratings described in the previous section, except in the case of the first test, where two test gratings not included in the recount (Sec 5.2.3) were used. Fibers used as gain medium in the cavities as well as amplifiers were again Ytterbium doped DC fibers (LIEKKI™ Yb1200-6/125 DC). According to simulations and common theory, the aim was to find a balance between short cavity length, in order to achieve high longitudinal mode spacing, and long cavity length to increase pump absorption in the cavity. In the end, cavity length was limited by the splicing and cleaving equipment and my own (lack of) experience resulting in cavity lengths of about 10 cm. Simulations made for this length indicated this should be short enough to produce stable single mode fiber lasers using 80% reflectivity output coupler gratings, i.e. lasers without or with low amount of mode-hops or polarization beating.

5.2.4.1 Test Laser 1

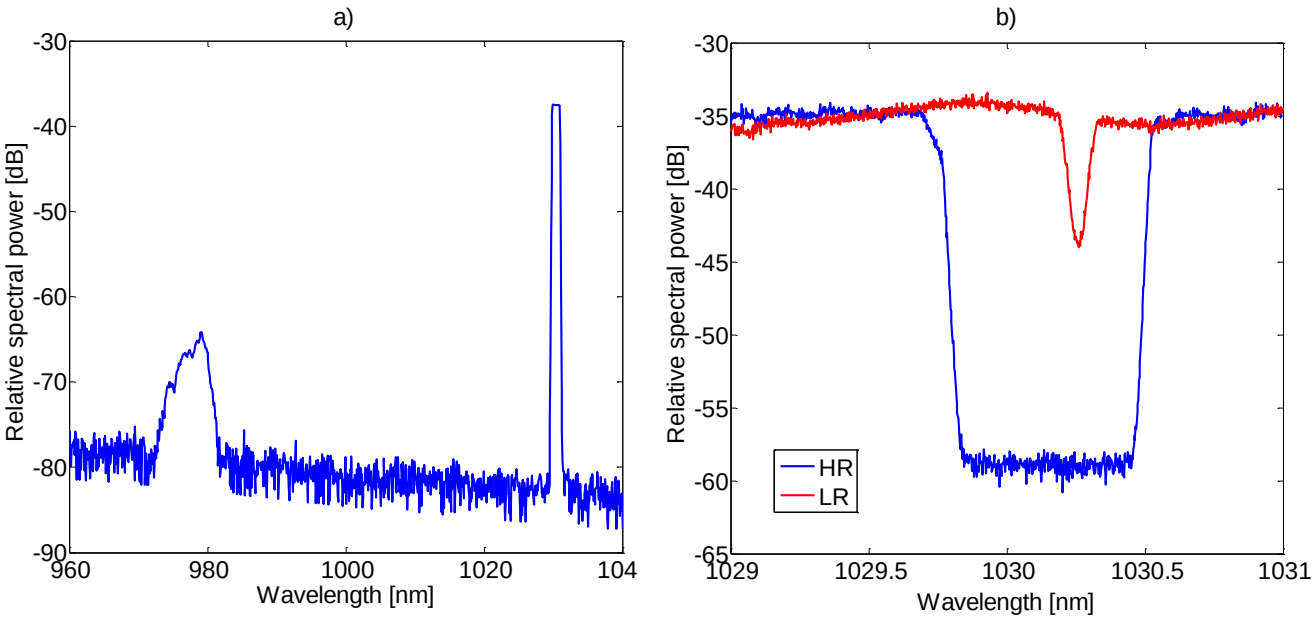

Figure 5.8: Spectral properties of Test Laser 1 (a), and the high- and low reflective (HR,LR) gratings used in its construction (b).

The HR grating used had a central wavelength of 1030.15 nm and a zero-to-zero bandwidth of 0.696 nm. The LR grating was centred at 1030.26 nm with a bandwidth of 0.079 nm. Figure 5.8 shows the spectra of the gratings used and the resulting laser spectrum. There is a relatively high amount of pump light left in the beam since no active fiber was used to absorb this after the output and the dichroic mirror used as filter was unable to entirely separate pump from signal.

In this first test an output power of 40mW was achieved without amplification at the central wavelengh of 1030.35nm. Unfortunately a bad splice caused a fiber fuse at the low reflective grating during normal operation at high (~8W) pump power destroying the laser.

5.2.4.2 Test Laser 2

Since all the gratings were written in single mode fiber, which effectively couples large amounts of light into the surroundings if they are in contact with anything but air It was necessary to always splice the lasers to some kind of pump delivery fiber and an output fiber in order to fix their positions.

The available passive output fibers were 105 µm core fibers. This caused concern for beam profile degradation. As light travelled along this non-single mode 105 µm fiber the laser mode field would eventually evolve into transversal multimode. Therefore, the choice was made to use available active 6/125 µm Yb-fiber as output fiber. This would in effect also amplify the laser signal without tests being made on the unamplified seed.

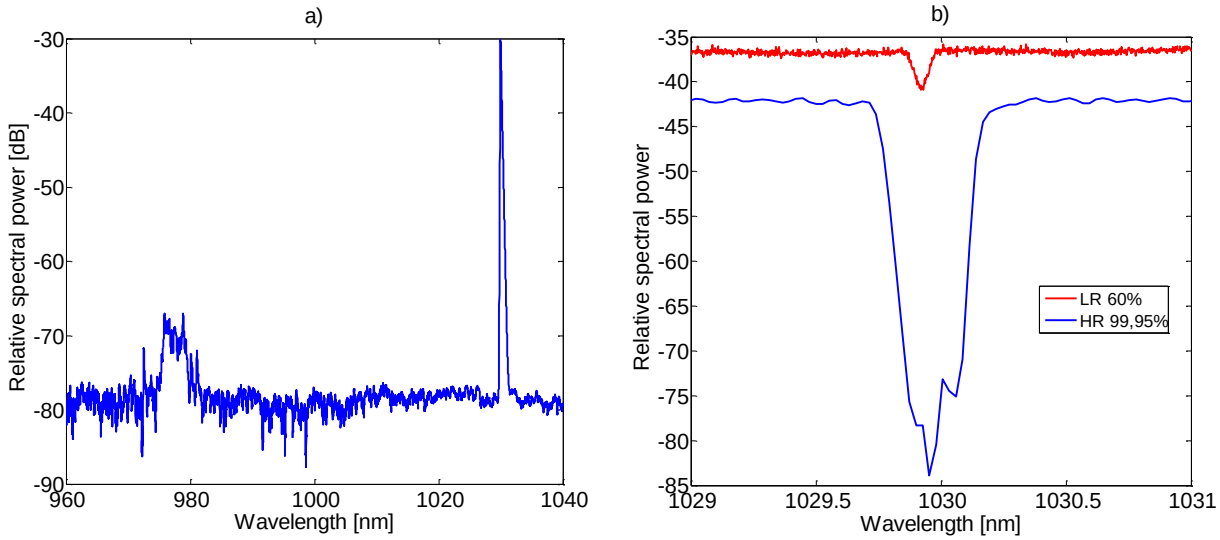

Figure 5.9: Spectral properties of Test Laser 2 (a), and the high- and low reflective (HR,LR) gratings used in its construction (b).

The second laser constructed utilized FBG #11, centred at 1029.925nm with a bandwidth of 0.08nm as the cavity output coupler and FBG #20 with central wavelength at 1029.956nm and a bandwidth of 0.4nm as the cavity end mirror. Fig. 5.9 shows the spectral properties of the gratings used in its construction as well as the resulting laser spectrum.

This second laser delivered output powers as high as 1.1W using ca 5 meters of amplification fiber and a pump power of 8W. The central wavelength can be located at 1029.936 nm which corresponds well to the peak of the low reflectivity grating if there is a slight thermal drift (Which should be present). Some pump light can still be detected in the output beam, but it is almost 40dB lower in power than the signal.

5.2.4.3 Lasers for full prototype setup

A severely limiting factor in the handling of the gratings and lasers up to this point was the existence of pieces of bare single mode fiber. These pieces were not only sensitive to light loss on contact with other materials but also had a much lower mechanical strength. This forced the need for as little movement of any setup as possible. Therefore, the decision was made to try and splice and mount the whole setup in place, instead of a modular construction that could be assembled later but risking damage due to more handling.

The gratings chosen for the three lasers are shown in table 1. Bandwidth is the zero-to-zero bandwidth and not FWHM.

Table 1

Nr	Central wavelength [nm]	Bandwidth [nm]	Reflectivity
25	1029.13	0,072	67%
17	1029.2	0,78	99.9%
27	1030.02	0,082	83%
22	1030.1	0,72	99.9%
14	1031.43	0,098	82%
13	1031.2	0,85	99.8%

Each laser was spliced onto one of the three arms of the splitter (described in Sec. 5.2.2) and to approximately 3m of Yb-doped fiber on the output end. Each piece was fixed in place as soon as it was practically possible to reduce the risk of stress damage and mistakes in handling.

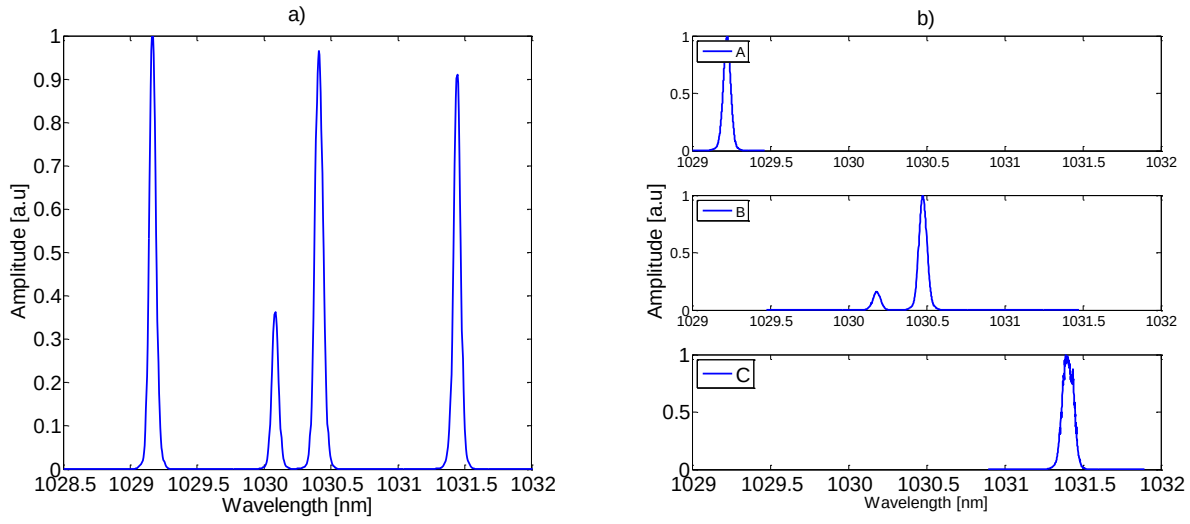

Figure 5.10: (a) Spectrum of three lasers pumped from single source at (near) equal lasing output power. (b) Individual spectrum of each laser.

The spectral properties of the three lasers were recorded by an optical spectrum analyser, both collectively and separately as shown in Fig.5.10. Near equal output power was achieved thanks to the use of free space methods to illuminate the splitter and get an optimum balance between even pow-

er distribution between the lasers and maximum total output power. In principle, the lasing wavelengths were mainly determined by λ_B of the narrow gratings, verified by laser A (1029.22 nm) and laser C (1031.4 nm). The small differences between the signal wavelengths and the measured λ_B at room temperature can be attributed to temperature induced wavelength shifts. However, laser B has two peaks (1030.18 nm and 1030.48 nm), which can possibly be attributed to either bad splicing or some stress-induced damage in the grating. Nonetheless, the conviction is that this technical issue can be resolved in the future.

5.2.4.4 M^2 and Coherence and Mode characteristics

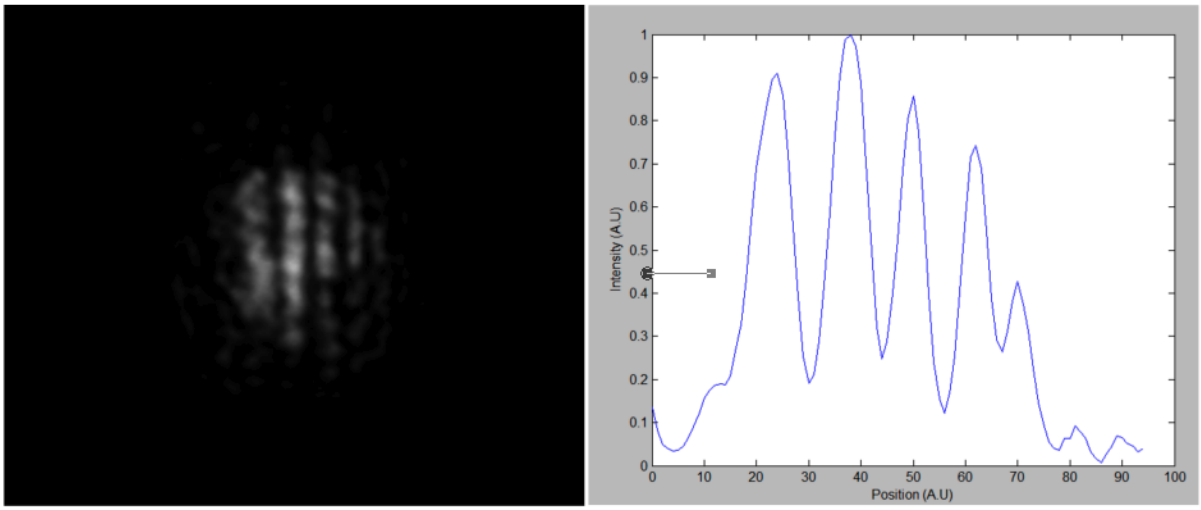

Figure 5.2: Interference pattern at 10m (left) of the 1029nm laser, and corresponding intensity profile (Right). The resulting visibility is at 60%, i.e. far from the lower boundary of laser beam interference visibility of 37% defining actual coherence length.

Several reasons made results from M^2 measurements using knife edge technique [22] difficult to interpret. One reason was the power fluctuations of both pump and signal. Another issue was the performance of the power meters under the effect of heating, initial measurements of 450mW would easily fall to 300mW or lower after a few minutes. Therefore M^2 values ranging from 1.3 all the way up to 4 could be calculated for the same laser.

Attempts to measure the mode characteristics of the lasers using Fabry-Perrot interferometers likewise yielded inconclusive results, meaning that attempted F-P measurements suggested the presence of four to eight longitudinal modes. However, these could never be stabilized to get a clear reading or snapshot. It has later been confirmed this was due to damaged electronics. New measurements could not be made since the prototype was already shipped to the end user at LTU.

More importantly, narrow linewidth operation for the lasers could be verified by determining their coherence lengths by simple interferometric measurements using a common Michelson setup. The lasers had coherence length well above 10 m, suggesting bandwidths below 3 MHz (or 10.6 fm), well within the requirement for holographic measurements. Such a low bandwidth suggests few modes which in turn implies low values of M^2

6 Results

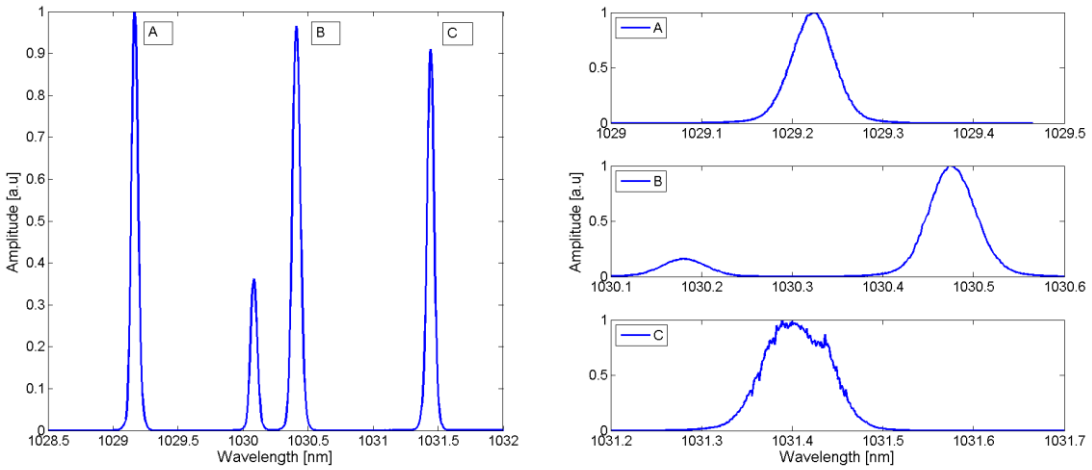

Figure 6.1(Left) Spectrum of three lasers pumped from single source at (near) equal lasing output power. (Right) Individual spectra of the three lasers.

The above figure shows the end result measurements of the three lasers, both taken separately and collectively. Near equal output power was achieved using free space mechanics to illuminate the splitter and get an optimum balance between even power distribution between the lasers and maximum total output power. The main advantage of this free space setup was the ability to manipulate output power despite using non identical fiber gratings, cavity lengths and amplification. At near 33/33/33% output the individual powers were measured to be very close to 457 / 451 / 452 mW for a total of 1.36W combined CW output.

Spectrally none of the lasers can be considered completely wavelength stable and simultaneous oscillation on several modes occur causing the wavelengths to fluctuate within a narrow, less than 0,06 nm wide band. This can of course be attributed to several possible reasons. Poor/unstable pump, mechanical instability in the setup, heat fluctuations or , in fact, low sensitivity optical spectrum analysers are all possible problems. Another very possible reason is an unstable polarization state since there is no polarizing or polarization maintaining components in the setup.

The side lobe of laser 2 is possibly due to some unwanted lasing on a side lobe of the grating and some fiber end surface or a bad splice. In fact, the weak grating of laser 2 is centred around 1030,02nm without considering heat shifts, causing the concern that this grating might be faulty or was destroyed during splicing. This suggests that the weak 1030,02 nm

grating gives rise to the small peak and lasing between the high reflectivity grating and a fiber end surface is what gives rise to the main peak around 1030,45 nm.

7 Future development

It was an early stated goal to always consider what future refinements could be made in case of an interest for further development. As such the constructed have plenty of areas that can be modified, changed or improved upon.

Pulsing is a main concern if the setup is to be used industrially. To ensure that the holographic snapshot of a surface is short enough not to record mechanical vibrations in a given sample measured pulse lengths need to be lower than 10 µs. This can for example be achieved using piezo electric elements. In a polarization maintaining fiber the reflection band of a FBG can be split by approximately 0.3 nm due to the different indexes of refraction in the fast and slow axis of a PM fiber. If birefringence is induced on a non-PM fiber using a piezo it is possible to control polarization in such a way that the fast axis reflection would be within the reflection band of the FBG while the slow axis would be located outside the reflection band [19]. Using this technique pulse energies of 54 µJ at 153 ns pulses have been demonstrated.

If power is scaled it might be of interest to investigate liquid cooling. While fairly straightforward it is nonetheless something that can further increase stability in high power applications.

Coiling techniques mentioned in section 2.3 of this work can be employed to facilitate the use of larger core fibers. This could be of interest if there is a need to scale power upwards or if shorter fibers are desired.

Beam combining is difficult and if the number of lasers should be increased it will be increasingly difficult to keep the outputs aligned. This can be helped using for example VBGs [23] to combine the beams.

Many other aspects can be investigated such as photonic crystal fibers, polarisation maintaining systems other pumping techniques or up scaling of the present one. All in all, there is much work to be done by the curious and inquisitive.

8 References

1. Meiners-Hagen, K., et al., *Multi-Wavelength Interferometry for Length Measurements Using Diode Lasers.* Measurement Science Review, 2009. **9**(1): p. 16-26.
2. Wada, A., M. Kato, and Y. Ishii, *Multiple-wavelength digital holographic interferometry using tunable laser diodes.* Appl. Opt., 2008. **47**(12): p. 2053-2060.
3. Mann, C.J., et al., *Quantitative phase imaging by three-wavelength digital holography.* Opt. Express, 2008. **16**(13): p. 9753-9764.
4. Silfvast, W.T., *Laser Fundamentals*2004: Cambridge University Press.
5. Hecht, E., *Optics*2002: Addison-Wesley.
6. A.W. Snyder, J.L., *Optical Waveguide Theory.* Chapman and Hall, 1983.
7. Koplow, J.P., D.A.V. Kliner, and L. Goldberg, *Single-mode operation of a coiled multimode fiber amplifier.* Opt. Lett., 2000. **25**(7): p. 442-444.
8. Othonos, A., et al., *Fibre Bragg Gratings*

Wavelength Filters in Fibre Optics, H. Venghaus, Editor 2006, Springer Berlin / Heidelberg. p. 189-269.

9. Erdogan, T., *Fiber grating spectra.* Lightwave Technology, Journal of, 1997. **15**(8): p. 1277-1294.
10. Paschotta, R., et al., *Ytterbium-doped fiber amplifiers.* Quantum Electronics, IEEE Journal of, 1997. **33**(7): p. 1049-1056.
11. Pask, H.M., et al., *Ytterbium-doped silica fiber lasers: versatile sources for the 1-1.2 μm region.* Selected Topics in Quantum Electronics, IEEE Journal of, 1995. **1**(1): p. 2-13.
12. Aleksoff, C.C. *Multi-wavelength digital holographic metrology*. 2006. San Diego, CA, USA: SPIE.
13. Aleksoff, C.C., *Multi-wavelength digital holographic metrology.* 2006: p. 63111D-63111D.
14. Daneu, V., et al. *Spectral beam combining of a broad-stripe diode laser array in an external cavity*. in *Lasers and Electro-Optics, 2000. (CLEO 2000). Conference on*. 2000.
15. Jun Zang, E., et al., *Single-frequency 1.25 W monolithic lasers at 1123 nm.* Opt. Lett., 2007. **32**(3): p. 250-252.
16. Nilsson, A.C., E.K. Gustafson, and R.L. Byer, *Eigenpolarization theory of monolithic nonplanar ring oscillators.* Quantum Electronics, IEEE Journal of, 1989. **25**(4): p. 767-790.
17. Mooradian, A. *High brightness cavity-controlled surface emitting GaInAs lasers operating at 980 nm*. in *Optical Fiber Communication Conference and Exhibit, 2001. OFC 2001*. 2001.
18. Griebner, U. and R. Koch, *Passively Q-switched Nd:glass fibre-bundle laser.* Electronics Letters, 1995. **31**(3): p. 205-206.
19. Shi, W., et al. *High-energy single-mode single-frequency all-fiber laser pulses covering C-band based on highly co-doped phosphate glass fibers*. 2009. San Jose, CA, USA: SPIE.
20. Ranaud, C.C., et al., *Characteristics of Q-switched cladding-pumped ytterbium-doped fiber lasers with different high-energy fiber designs.* Quantum Electronics, IEEE Journal of, 2001. **37**(2): p. 199-206.
21. Kashyap, R., *Fiber Bragg Gratings*1999: Elsevier Science.
22. Tjörnhammar, S., *Pulsed Yb:KYW laser and UV generation*, 2010. p. 61.

23. Andrusyak, O., et al. *External and common-cavity high spectral density beam combining of high power fiber lasers*. 2008. San Jose, CA, USA: SPIE.